The Jackson Laboratory

The Mouseion at the JAXlibrary

11-20-2023

Generation of glucocorticoid-producing cells derived from human pluripotent stem cells.

Gerard Ruiz-Babot

Ariane Eceiza

Fernando Abollo-Jiménez

Maria Malyukov

Diana L Carlone

See next page for additional authors

Original Citation

Ruiz-Babot G, Eceiza A, Abollo-Jiménez F, Malyukov M, Carlone D, Borges K, Da Costa A, Qarin S, Matsumoto T, Morizane R, Skarnes W, Ludwig B, Chapple P, Guasti L, Storr H, Bornstein S, Breault D. Generation of glucocorticoid-producing cells derived from human pluripotent stem cells. Cell Rep Methods. 2023;3(11):100627.
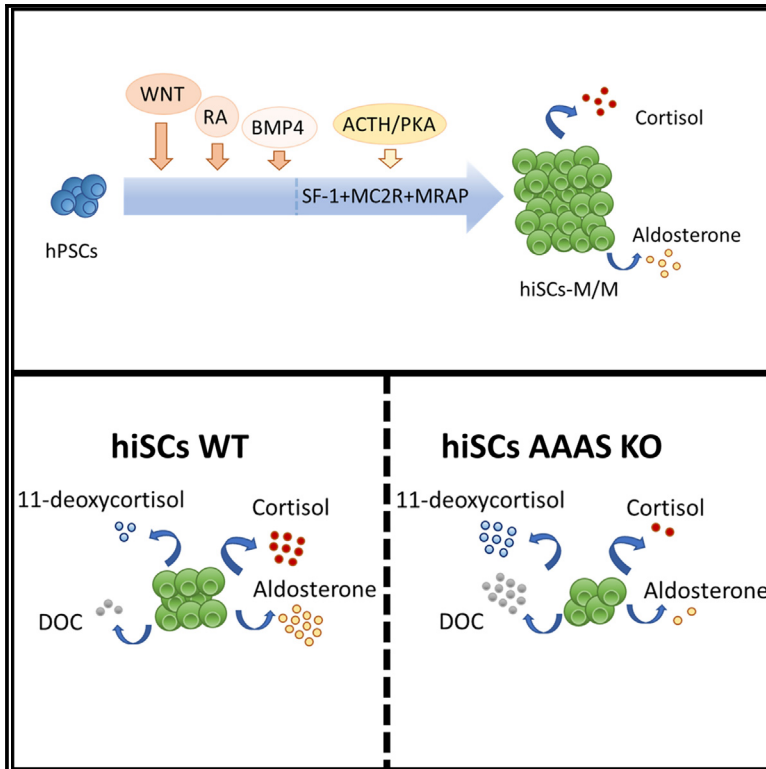
Authors

Gerard Ruiz-Babot, Ariane Eceiza, Fernando Abollo-Jiménez, Maria Malyukov, Diana L Carlone, Kleiton Borges, Alexandra Rodrigues Da Costa, Shamma Qarin, Takuya Matsumoto, Ryuji Morizane, William C Skarnes, Barbara Ludwig, Paul J Chapple, Leonardo Guasti, Helen L Storr, Stefan R Bornstein, and David T Breault

Generation of glucocorticoid-producing cells derived from human pluripotent stem cells

Graphical abstract

Authors

Gerard Ruiz-Babot, Ariane Eceiza, Fernando Abollo-Jiménez, ..., Helen L. Storr, Stefan R. Bornstein, David T. Breault

Correspondence

gerard.ruiz-babot@uniklinikum-dresden.de (G.R.-B.),
david.breault@childrens.harvard.edu (D.T.B.)

In brief

Ruiz-Babot et al. demonstrate generation of hiSCs from pluripotent stem cells. The resulting cells produce cortisol, respond to ACTH, and fail to undergo terminal differentiation. HiSCs are used to model triple A syndrome and represent a step toward cellular therapy for patients with AI.

Highlights

- Generation of human-induced steroidogenic cells from pluripotent stem cells

- Production of cortisol-producing and ACTH-responsive cells

- Lack of terminal differentiation allows for generation of large numbers of cells

- Modeling of triple A syndrome using differentiated cells

CellPress

Article

Generation of glucocorticoid-producing cells derived from human pluripotent stem cells

Gerard Ruiz-Babot,[1,2,3,11,*] Ariane Eceiza,[1,2] Fernando Abollo-Jiménez,[4] Maria Malyukov,[3] Diana L. Carlone,[1,2] Kleiton Borges,[1,2] Alexandra Rodrigues Da Costa,[5] Shamma Qarin,[6] Takuya Matsumoto,[7,9] Ryuji Morizane,[2,7,9] William C. Skarnes,[8] Barbara Ludwig,[3] Paul J. Chapple,[5] Leonardo Guasti,[5] Helen L. Storr,[5] Stefan R. Bornstein,[3,10] and David T. Breault[1,2,*]

[1]Division of Endocrinology, Boston Children's Hospital, Harvard Medical School, Boston, MA, USA
[2]Harvard Stem Cell Institute, Cambridge, MA, USA
[3]Department of Medicine, University Hospital Carl Gustav Carus, Dresden, Germany
[4]Maimonides Biomedical Research Institute of Cordoba (IMIBIC), Córdoba, Spain
[5]Centre for Endocrinology, William Harvey Research Institute, Bart's and the London School of Medicine and Dentistry, Queen Mary University of London, London, UK
[6]Wellcome-MRC Cambridge Stem Cell Institute, Cambridge Biomedical Campus, University of Cambridge, Puddicombe Way, Cambridge, UK
[7]Wyss Institute for Biologically Inspired Engineering, Harvard University, Cambridge, MA, USA
[8]Cellular Engineering, The Jackson Laboratory for Genomic Medicine, Farmington, CT 06032, USA
[9]Nephrology Division, Massachusetts General Hospital, Boston, MA, USA
[10]Division of Endocrinology, Diabetes and Nutritional Sciences, Faculty of Life Sciences and Medicine, King's College London, London, UK
[11]Lead contact
*Correspondence: gerard.ruiz-babot@uniklinikum-dresden.de (G.R.-B.), david.breault@childrens.harvard.edu (D.T.B.)
https://doi.org/10.1016/j.crmeth.2023.100627

MOTIVATION Adrenal insufficiency is a life-threatening condition resulting from the inability to produce steroid hormones in a dose and time-dependent manner. The ability to generate cells that produce cortisol in response to adrenocorticotrophic hormone (ACTH), the main regulator of glucocorticoid production in humans, combined with the development of encapsulation and immunoprotecting technologies, will open future opportunities to treat this condition using cell-based therapies. Current protocols have demonstrated the generation of fetal-like steroid-producing cells from hPSCs. However, the resulting cells fail to secrete cortisol, the main glucocorticoid in humans. We therefore sought to develop a protocol that enables the generation of billions of cells that produce cortisol and can respond to ACTH stimulation.

SUMMARY

Adrenal insufficiency is a life-threatening condition resulting from the inability to produce adrenal hormones in a dose- and time-dependent manner. Establishing a cell-based therapy would provide a physiologically responsive approach for the treatment of this condition. We report the generation of large numbers of human-induced steroidogenic cells (hiSCs) from human pluripotent stem cells (hPSCs). Directed differentiation of hPSCs into hiSCs recapitulates the initial stages of human adrenal development. Following expression of steroidogenic factor 1, activation of protein kinase A signaling drives a steroidogenic gene expression profile most comparable to human fetal adrenal cells, and leads to dynamic secretion of steroid hormones, *in vitro*. Moreover, expression of the adrenocorticotrophic hormone (ACTH) receptor/co-receptor (MC2R/MRAP) results in dose-dependent ACTH responsiveness. This protocol recapitulates adrenal insufficiency resulting from loss-of-function mutations in *AAAS*, which cause the enigmatic triple A syndrome. Our differentiation protocol generates sufficient numbers of hiSCs for cell-based therapy and offers a platform to study disorders causing adrenal insufficiency.

INTRODUCTION

Adrenal glands are essential for life and control fundamental physiological functions through the synthesis and secretion of cortisol and aldosterone, including regulation of volume status, salt homeostasis, and carbohydrate metabolism, and are a central medi-ator of the physiological stress response. The inability to produce adrenal steroids results in adrenal insufficiency (AI), a life-threatening disorder.[1] Current treatments consist of replacement of the missing hormones; however, this approach has three main limitations: inappropriate glucocorticoid substitution leads to unwanted side effects; hormone replacement cannot mimic the
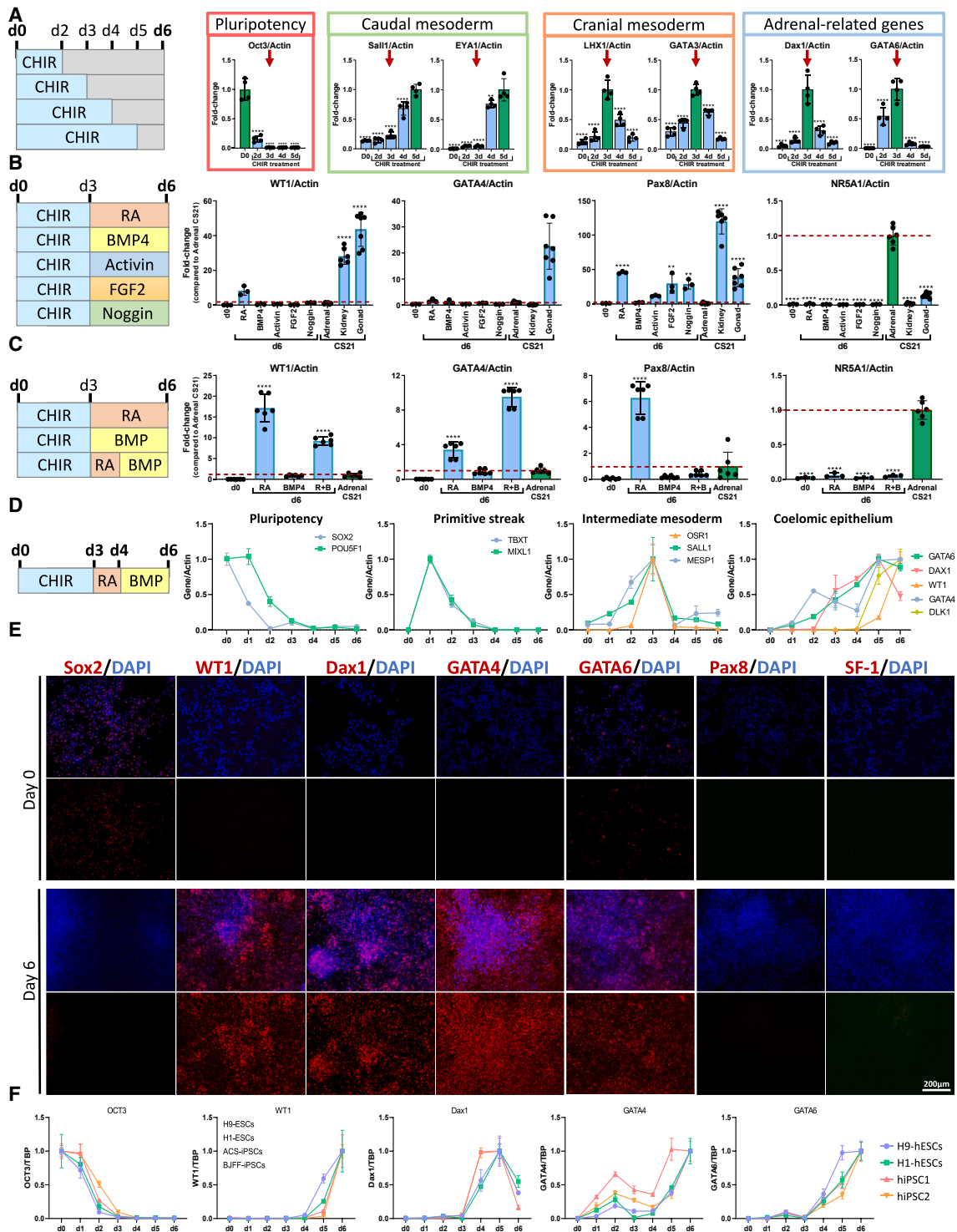
Figure 1. Differentiation of hPSCs into adrenal precursor-like cells

(A) RT-qPCR analysis of pluripotency, caudal mesoderm, cranial mesoderm and adrenal-related genes of hPSCs treated with CHIR 3 μM for 2, 3, 4, and 5 days. After the period of incubation with CHIR, medium was replaced with AdvRPMI+GlutaMAX+P/S until day 6.

(B) RT-qPCR analysis of hPSCs treated for 3 days with CHIR 3 μM and for 3 days with either RA 1 μM, BMP4 10 ng/mL, Activin 10 ng/mL, FGF2 10 ng/mL, or Noggin 10 ng/mL. Gene expression was compared with adrenal, kidney, and gonads at CS21. Dotted line corresponds with the mean expression levels of adrenal cDNA at CS21.

(legend continued on next page)

physiological circadian rhythm of glucocorticoid release; and stress-induced secretion of glucocorticoids cannot be achieved with current medications. Alternatively, cell-based replacement strategies offer the promise of greater precision, decreased morbidity, and improved safety for the treatment of AI patients.

We and others have generated steroidogenic cells using directed differentiation and reprogramming strategies with a variety of starting cell types including fibroblasts,[2,3] mesenchymal stem cells,[4–12] embryonic stem cells (ESCs)[12–15] and induced pluripotent stem cells (iPSCs).[15–17] While these approaches have enabled modeling of human diseases affecting the adrenal cortex, such as congenital adrenal hyperplasia (CAH),[6] their tendency to induce non-proliferative, terminally differentiated steroidogenic cells upon reprogramming makes them unsuitable for cell-based therapies, which require billions of cells per patient.

The adrenal glands develop from the intermediate mesoderm (IM), a group of cells that arise and migrate from the embryonic primitive streak upon Wingless and Int-1 (WNT) pathway activation.[18,19] Retinoic acid (RA) is a well-known factor involved in the regulation of the antero-posterior and left-right patterning of the embryo,[20] playing a role in rostral IM specification in early development. During adrenal development, RA pathway proteins are expressed early, and decrease as the organs matures.[21] Bone morphogenic protein (BMP) signaling regulates intermediate and lateral mesoderm gene expression, in a dose-dependent manner, both *in vitro* and *in vivo*.[22] The combined modulation of these signaling pathways has been applied to human pluripotent stem cells to generate nephrogenic IM[23] and more recently human fetal zone adrenal-cortex-like cells.[16]

Robust differentiation protocols also allow for modeling human conditions where the underlying mechanisms remain poorly defined. Allgrove or triple A syndrome is a congenital human autosomal recessive disorder characterized by alacrima, achalasia, and AI, as well as neurodegeneration and autonomic dysfunction.[24] Triple A syndrome is caused by mutations in *AAAS*,[25] which encodes ALacrima Achalasia aDrenal Insufficiency Neurological (ALADIN) disorder, a WD-repeat protein localized in the nuclear pore complex. In humans, unlike mice, the lack of ALADIN leads to reduced viability of steroidogenic cells due to increased susceptibility to oxidative stress and alteration of redox homeostasis, as well as impaired steroidogenesis through downregulation of key steroidogenic enzymes.[26,27] Precisely how ALADIN deficiency mediates these changes remains to be established.

Here, we report the generation and expansion of human-induced steroidogenic cells (hiSCs) from human pluripotent stem cells (hPSCs) through the development of a directed differentiation protocol, that does not induce terminal differentiation, using activators of WNT, RA, and BMP signaling pathways. Upon viral expression of steroidogenic factor 1 (SF-1), hiSCs secrete cortisol, which is enhanced upon activation of protein ki-

nase A (PKA) signaling. Single-cell gene expression analysis reveals that hiSCs exhibit a molecular signature that most closely resembles a 12-week human fetal adrenal. Upon expression of MC2R and MRAP, adrenocorticotrophic hormone (ACTH) receptor and co-receptor, respectively, hiSCs can respond to ACTH in a dose-dependent manner. Finally, *AAAS*-null human iPSCs (hiSPCs) exhibit reduced secretion of glucocorticoids and mineralocorticoids, compared with controls. This is consistent with AI in triple A syndrome patients, confirming the utility of this protocol to model adrenal disease.

RESULTS

Characterization of human adrenal, gonadal, and kidney development *in vivo*

Given that directed differentiation of hPSCs into mature adrenal cells will likely require recapitulation of normal development, we analyzed gene and protein expression during human adrenal formation, from early embryonic Carnegie stages (CS), through fetal post-conception weeks (pcw) 14–21, to adulthood (Figure S1A). We first established the relative expression pattern of selected genes across human adrenal development from CS19 through adulthood using RT-qPCR (Figure 1A). *NR5A1* (the gene encoding SF-1) and *DAX1*, two critical transcription factors for adrenal development,[28,29] show a modest increase from early development to adulthood (Figure S1A). Similarly, genes encoding steroidogenic enzymes (*StAR, CYP11A1, CYP11B1,* and *CYP11B2*), the ACTH receptor (*MC2R*) and co-receptor (*MRAP*) are expressed at low levels during early embryonic stages and increase with development into fetal and adult stages (Figure S1A). In contrast, *WT1* (the gene encoding Wilms tumor 1) is expressed at relatively higher levels during the initial stages of adrenal development (Figure S1A), albeit with some variability, consistent with its role in specifying adrenal identity,[30] followed by a marked decrease in expression from pcw 18 through adulthood, where WT1 levels are almost undetectable (Figure S1A).

As adrenal glands, gonads, and kidney arise from the IM,[19] we next performed gene and protein expression profiling of key factors involved in the development of human embryonic and fetal adrenals, gonads, and kidneys at different stages of development (Figures S1B and S1C). Such markers can then be used during the design of differentiation protocols to help describe the impact of specific perturbations on lineage development into each of these three tissues. RT-qPCR analysis revealed expression of *CYP11B1, CYP11B2, MC2R,* and *MRAP* exclusively in adrenal tissue (Figure S1B), consistent with their established roles during adrenal development and steroidogenesis in adulthood.

To gain more insight into the spatial and temporal patterning of these markers, we next performed an immunofluorescence analysis (Figure S1C). Shortly after the adrenal and gonadal

(C) RT-qPCR analysis of hPSCs treated for 3 days with CHIR and combinations of BMP4 and RA for 3 days. Gene expression was compared with adrenal at CS21.
(D) Time course analysis of gene expression by RT-qPCR of pluripotency, primitive streak, IM, and adrenal development genes.
(E) Immunocytochemistry of pluripotency and early adrenal development genemarkers at the beginning (d0, top) and end of differentiation (d6, bottom) of a hESC line after 3 days of CHIR, 1 day of RA and 2 days of BMP4. DAPI (in blue) indicates nuclear staining. Scale bar, 200 μm.
(F) Time course analysis of gene expression by RT-qPCR of pluripotency (OCT3) and early adrenal development (WT1, DAX1, GATA4, and GATA6) markers from 2 hESC lines and 2 iPSC lines. All data are represented as mean ± SEM. Green bars depict the column used for comparison to other bars. Statistical significance was determined using one-way ANOVA followed by Dunnet's multiple comparison test correction. See also Figures S1–S3.
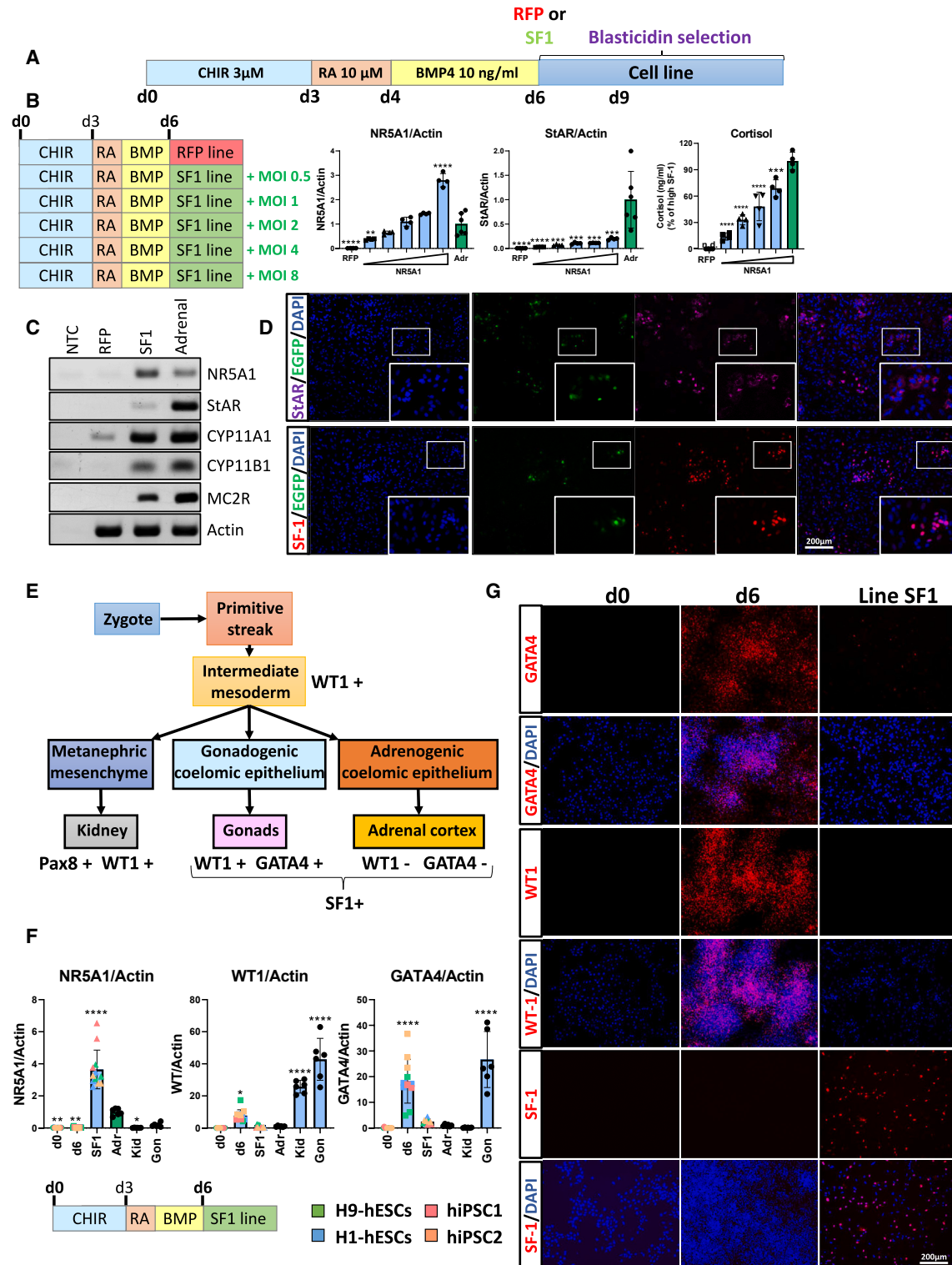
Figure 2. Generation of human induced steroid-producing cells (hiSCs) from adrenal precursor-like cells

(A) Overview of the protocol to generate hiSCs.

(B) Generation of cell lines with different doses of NR5A1 (SF-1). Differentiated cells were infected with NR5A1-expressing lentivirus at an MOI of 0.5–8, selected with blasticidin, followed by analysis of gene expression (compared with adrenal at CS21) and cortisol secretion analyzed by ELISA.

(C) Endpoint PCR analysis of NR5A1, StAR, CYP11A1, CYP11B1, and MC2R.

(legend continued on next page)

primordium are specified (CS15–17), adrenal cells express the transcription factor SF-1 and, at low levels, the transcription factor WT1, as shown in Figures S1C and S2A. WT1 and SF-1 expression are essential to define the AGP.[28,30] While expression of WT1 persists in the developing gonads and mesonephros and kidneys, its expression is downregulated in the adrenals during early development (Figures S1B, S1C, and S2A). In contrast, SF-1 continues to be expressed throughout adrenal development into adulthood (Figures S1A–S1C). In the adult, WT1 is highly expressed in gonads and kidney while absent in the adrenals (Figures S1B and S1C). The transcription factor GATA4 is required for formation of the urogenital ridge in mice[31] and later in development marks gonadal tissue.[31] In contrast, GATA4 expression is reduced in mouse adrenal, mesonephros, and kidney.[30,32] Consistent with data from the mouse, GATA4 expression was not detected in adrenals and mesonephros/kidneys (Figures S1B and S1C). The transcription factor PAX8 is expressed in the developing mesonephros and kidney and in supporting cells of the gonads but is absent in developing adrenal[33,34] (Figures S1B and S1C). Analysis of steroidogenic acute regulatory protein (StAR), the rate-limiting enzyme required for steroidogenesis, revealed expressed in adrenal and testis, but not in the ovary (Figures S1B and S1C). Interestingly, DLK1, a marker of undifferentiated human adrenal progenitor cells,[35] is highly expressed in the embryonic adrenal gland and expressed at lower levels in the other tissues (Figures S1B and S2B). Finally, the RA-producing enzyme, ALDH2A1, is expressed in the developing adrenal and expression decreases with organ maturation (Figure S2C), as described previously.[21] Taken together, these data provide critical spatial and temporal information for determining the pattern and timing of factors important for adrenal, gonadal and kidney development (Figure S2D).

Generation of adrenal precursor-like cells (coelomic epithelial-like cells)

The adrenal and the gonad arise from the cranial IM. To generate cells resembling the precursors of the adrenogenic coelomic epithelium, we first sought to differentiate the H9 human ESCs (hESCs) line toward IM by activating canonical WNT signaling, which governs the cranial/caudal axis of the embryo.[36,37] Longer exposure to WNT signaling leads to caudalization, whereby cells that migrate cranially receive less exposure to WNT signals.[18] Canonical WNT signaling is, therefore, required for differentiation of pluripotent stem cell-derived mesoderm in vitro.[38] Based on this, we first performed a 6-day time course analysis treating hESCs for 2–5 days with the GSK3β inhibitor CHIR99021 at 3 μM (CHIR, an activator of canonical WNT signaling), followed by analysis of gene expression. Just 2 days of exposure to CHIR was sufficient to decrease expression of the pluripotency marker OCT3. In contrast, caudal IM markers, such as EYA1 and SALL1,[18,39] peaked after 5 days of exposure. Notably, cranial mesoderm markers, such as LHX1 and GATA3, as well as adrenal transcription factors, such as DAX1 and GATA6, peaked after 3 days of exposure (Figures 1A and S3A).

Homeobox (HOX) genes play a crucial role in specifying cell identity and positioning during embryonic development. In mice, the adrenal glands arise from cells that express HOX genes 5–9,[40] while the adult kidney (a more caudal structure) is specified by expression of HOXD11[41] (Figure S3B). As predicted, exposure to CHIR for more than 3 days drives cells toward a caudal phenotype, specified by expression of HOXA9, HOXB9, and HOXD9 (Figure S3A). With just 3 days of exposure to CHIR, cells show an adrenal HOX gene signature, specified by expression of HOXB4, HOXC6, and HOXA7 (Figure S3A). Taken together, these data show that the gene expression profile after 3 days of CHIR is similar to the one described in mice.[40]

We next assessed the impact of a variety of morphogens including RA, BMP4, activin A, fibroblast growth factor 2 (FGF2) and Noggin, known to be involved in urogenital ridge specification,[42] on hESCs after CHIR treatment (days 0–3). To distinguish between factors leading to adrenal, gonadal, and kidney development, we assessed gene expression of WT1 (kidney/gonad), GATA4 (gonad), PAX8 (kidney/gonad), and NR5A1 (adrenal) using CS21 embryonic adrenal, gonadal, and kidney samples as positive controls. Treatment of cells from days 3 to 6 with each molecule, except BMP4 led to induced expression of PAX8, while only RA induced expression of WT1 and PAX8 (Figures 1B and S3C). In contrast, no molecules induced expression of GATA4 or NR5A1 (Figure 2B). Since transient expression of WT1 is required for adrenal formation,[30,43] we next assessed the impact of shorter exposure of RA following by exposure to BMP4 (Figures 1C and S3D). Remarkably, treatment with CHIR from days 0 to 3, followed by RA from days 3 to 4 and BMP4 from days 4 to 6 induced expression of WT1 without inducing PAX8. GATA4 was also induced following exposure to RA and RA+BMP4, but not BMP4 alone (Figures 1C and S3D). Time course expression analysis showed a decrease in pluripotency markers (SOX2 and OCT3) by days 1–2, a peak in primitive streak markers (TBXT and MIXL1) on days 1–2, a peak in IM markers (OSR1, SALL1, and MESP1) by day 3 and a steady increase in genes present in the coelomic epithelium (GATA6, DAX1, WT1, GATA4, DLK1, and STAR) from days 2 to 6 (Figure 1D). Gene expression results were confirmed at the protein level with immunostaining for the pluripotency marker SOX2, the AGP markers WT1, DAX1, GATA4, and GATA6, and the kidney marker PAX8 (Figure 1E). Consistent with the gene expression data (Figure 1C), we were unable to detect expression of SF-1 (Figure 1E).

To assess the reproducibility of this protocol (CHIR-RA-BMP4) with additional pluripotent cell lines, we then utilized the H1 hESC line as well as two hiSPC lines (hiPSC1 and hiPSC2). Time course analysis for gene expression (OCT3, WT1, GATA4, GATA6, and

(D) Immunocytochemistry for StAR, SF-1, and EGFP from lentivirus transduced NR5A1-IRES-tGFP$_{nuc}$ cells. DAPI (in blue) indicates nuclear staining. Scale bar, 200 μm.

(E) Schematic of different stages of adrenal, gonad, and kidney development.

(F) RT-qPCR analysis of undifferentiated hPSCs (d0), adrenal precursor-like cells (d6), or SF-1-transduced lines for NR5A1, WT1, and GATA4. Gene expression was compared with adrenal, kidney, and gonads at CS21.

(G) Immunocytochemistry for GATA4, WT1, and SF-1 from samples analyzed in F. DAPI (in blue) indicates nuclear staining. Scale bar, 200 μm. NTC, no template control. All data are represented as mean ± SEM. Green bars depict the column used for comparison to other bars. Statistical significance was determined using one-way ANOVA followed by Dunnet's multiple comparison test correction. See also Figure S4.
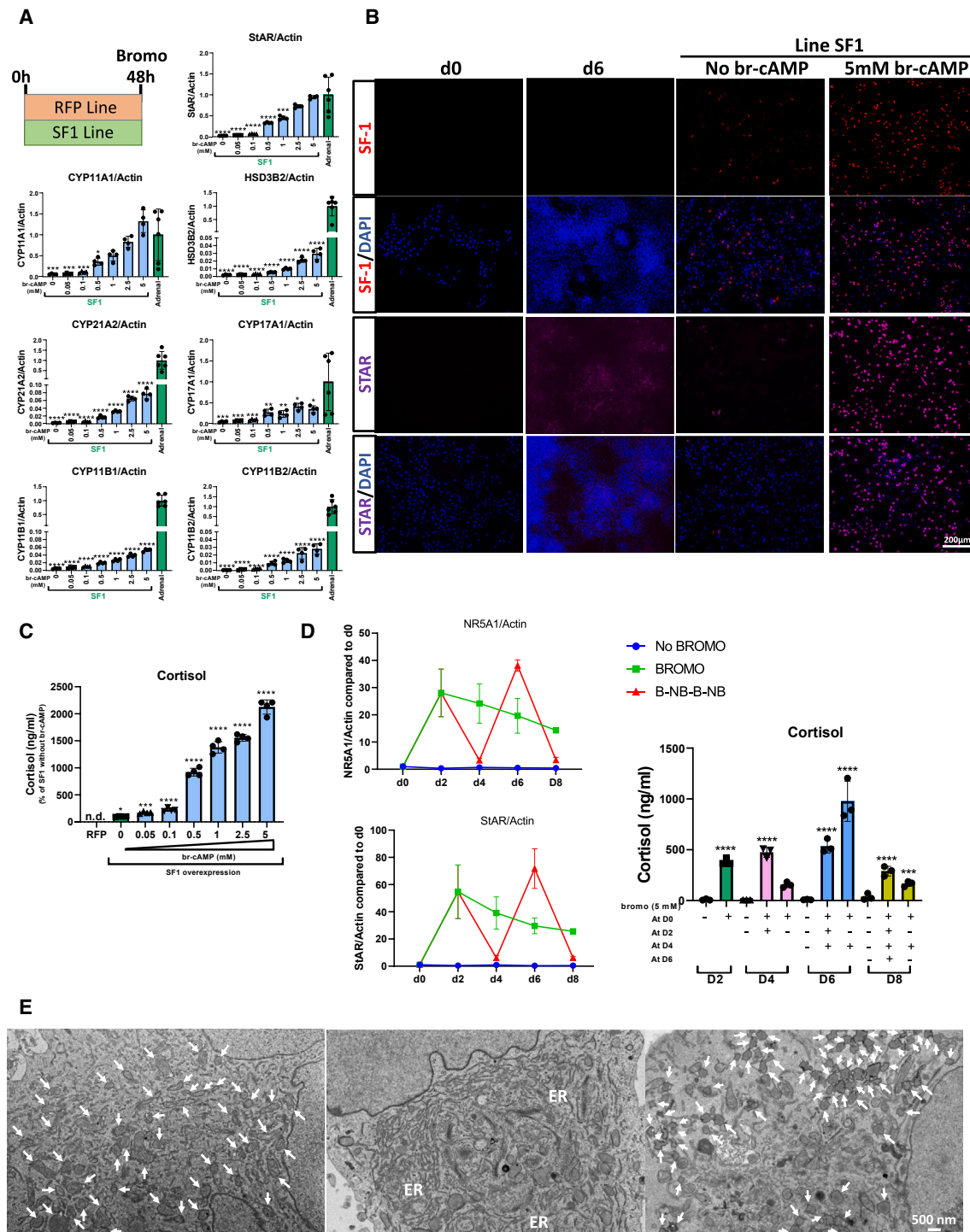
Figure 3. PKA signaling enhances steroidogenic properties of hiSCs

(A) RT-qPCR analysis of hiSCs unstimulated or stimulated with 0.05–5 mM bromo-cAMP (br-cAMP). Gene expression was compared with cDNA obtained from human adult adrenals.

(B) Immunocytochemistry for SF-1 and StAR of undifferentiated hPSCs (d0), adrenal precursor-like cells (d6) , and SF-1-transduced lines, untreated or treated with 5 mM br-cAMP for 48 h. DAPI (in blue) indicates nuclear staining. Scale bar, 200 μm.

(C) Cortisol secretion of mock and SF-1 transduced hiSCs treated with different concentrations of br-cAMP, analyzed by ELISA.

(legend continued on next page)

DAX1) as well as protein expression (SOX2, WT1, DAX1, GATA4, GATA6, PAX8, and SF-1) were comparable between all lines (Figures 1F and S3E).

Overall, the combination of CHIR for 3 days, RA for 1 day, and BMP4 for 2 days resulted in a reproducible protocol that generates cells with markers of early adrenal development using both human embryonic and iPSC lines.

Generation of steroid-producing cell lines

Despite the ability of our 6-day differentiation protocol to induce expression of genes and proteins involved in early adrenal development, we were unable to induce expression of *NR5A1* (SF-1), a master transcriptional regulator of steroidogenic cells, that is required for adrenal development[28] (Figures 1B, 1C, and 1E). To address this issue, we employed a lentiviral expression vector encoding NR5A1-IRES-tGFP to allow for graded express of SF-1 in our culture system, as a function of multiplicity of infection (MOI). A lentivirus expressing red fluorescent protein (RFP) was used as a control. Cells were infected with lentivirus at day 6 of differentiation, and three days after transduction cells were treated with blasticidin to select for transduced cells (Figures 2A and S4A). The resulting lines, regardless of the hPSC of origin, were called hiSCs.

Next, we performed a dose-response study, using increasing doses (MOI) of NR5A1 lentiviral particles to assess the effect of SF-1 expression levels on the ability of these cells to express cortisol, one of the major steroids produced by the adrenal cortex. Increasing doses of NR5A1 lentiviral particles increased the levels of StAR and the production of cortisol in a dose-dependent manner (Figure 2B). Consistent with induction of a steroidogenic program, RT-qPCR analysis revealed expression of most of the necessary steroidogenic enzymes (Figure 2C), while they are barely expressed in non-infected or control cell lines (Figures S3C and S4B). SF-1 and StAR were also detected at the protein level (Figure 2D). Note that the expression of SF-1 is slightly different between cells, depending on how much virus infected each cell (Figure S1C).

Adrenocortical cells, unlike gonadal cells, downregulate WT1 and GATA4 after lineage commitment (Figure 2E). Therefore, we next assessed the adrenal and/or gonadal gene and protein expression of these lineage-specific markers, comparing them with the endogenous levels in developing adrenal, gonad, and kidney at CS21. While WT1 and GATA4 are expressed at day 6 of differentiation for both hESCs and hiSPCs-derived hiSCs, upon induction of SF-1 expression and cell line generation, these levels decreased dramatically, consistent with the expression pattern observed in the adrenal gland at CS21 (Figure 2F). Gene expression results were corroborated at the protein level (Figure 2G).

The cholesterol needed for steroidogenesis is stored, in part, in lipid droplets within the cell.[44] SF-1-expressing hiSCs contain high numbers of lipid droplets, as assessed by Nile Red staining (Figure S4D). Importantly, these cells were not terminally differentiated, as evidenced by their ability to still divide, assessed

by Ki67 staining (Figure S4E). hiSCs were expanded for at least six passages without evidence for a decrease in their doubling time of approximately 28 h. Based on these results we extrapolate that more than 1 billion cells could be generated from a starting population of 15,000 hPSCs (Figure S4F).

Stimulation of steroidogenesis with PKA activators

Despite expressing SF-1 at levels that are comparable, if not several fold higher than native adrenal tissue (Figure 2B), hiSCs only produce moderate levels of StAR and steroidogenic enzymes (Figures 2B, 3C, and 3D). Adrenal cells regulate hormone production through ACTH-dependent stimulation of PKA signaling. Induction of PKA signaling in steroidogenic tissues has been shown to facilitate steroidogenesis by induction of StAR and activation of cyclic AMP (cAMP)-response elements (CRE) in promoters of steroidogenic genes.[45,46] In addition to the effects of PKA activation on steroidogenic enzymes, cAMP response elements in the SF-1 expression vector also contribute to enhanced expression of SF-1 in our system, in a dose-dependent manner (Figure S5A). This is likely due to the presence of four CRE-binding sites within the cytomegalovirus (CMV) promoter of the NR5A1-IRES-tGFP vector[47] (Figure S3A).

Consequently, stimulation with br-cAMP led to a dose-dependent increase in the expression of StAR and steroidogenic enzymes (Figure 3A), which was confirmed at the protein level (Figure 3B). Moreover, the levels of cortisol produced by the cells also increased in a dose-dependent fashion (Figure 3C). All adrenal-produced hormones and precursors were detected in the supernatant from hiSCs stimulated with br-cAMP (hereafter called br-hiSCs), assessed by liquid chromatography mass spectrometry (LC-MS) (Figure S5B), from different lines of hPSCs in independent experiments.

Next, we hypothesized that the serial addition and withdrawal of br-cAMP to hiSCs would dynamically regulate the levels of steroidogenic enzymes and hormone secretion. To test this, we added or removed br-cAMP to differentiated hiSCs for periods of 48 h, which confirmed that expression of steroidogenic enzymes, as well as cortisol production, is dynamically regulated by PKA activation (Figures 3D and S5D). In addition, exposure to br-cAMP led to a dramatic change in cell shape, with a decrease in cytoplasm and a stellate morphology (Figure S5D). To assess viability, cells were subjected to a live-dead assay, which revealed treatment with high concentrations of br-cAMP at 5 mM did not affect viability (Figure S5C). Electron microscopy of br-hiSCs revealed a high content of mitochondria (Figure 3E, left), endoplasmic reticulum (Figure 3E, middle), and lipid droplets (Figure 3E, right), all essential organelles for steroidogenesis.

RNA sequencing of PSCs-derived hiSCs

To further characterize hiSCs, undifferentiated hPSCs (d0 of differentiation), RFP-transduced cells unstimulated with br-cAMP (RFP) or stimulated with br-cAMP (br-RFP), hiSCs and br-hiSCs

---

(D) Dynamic regulation of gene expression (NR5A1 and StAR) and cortisol production of hiSCs treated with br-cAMP 5 mM hiSCs were treated or withdrawn from br-cAMP for 48-h windows. All data are compared with the first column (day 2 without br-cAMP treatment) for statistical analysis.
(E) Electron micrographs of br-hiSCs revealing mitochondria (arrow) (left), endoplasmic reticulum (ER) (middle) and lipid droplets mitochondria (arrow) (right). Scale bar, 500 nm. All data are represented as mean ± SEM. Green bars depict the column used for comparison to other bars. Statistical significance was determined using one-way ANOVA followed by Dunnet's multiple comparison test correction. See also Figure S5.
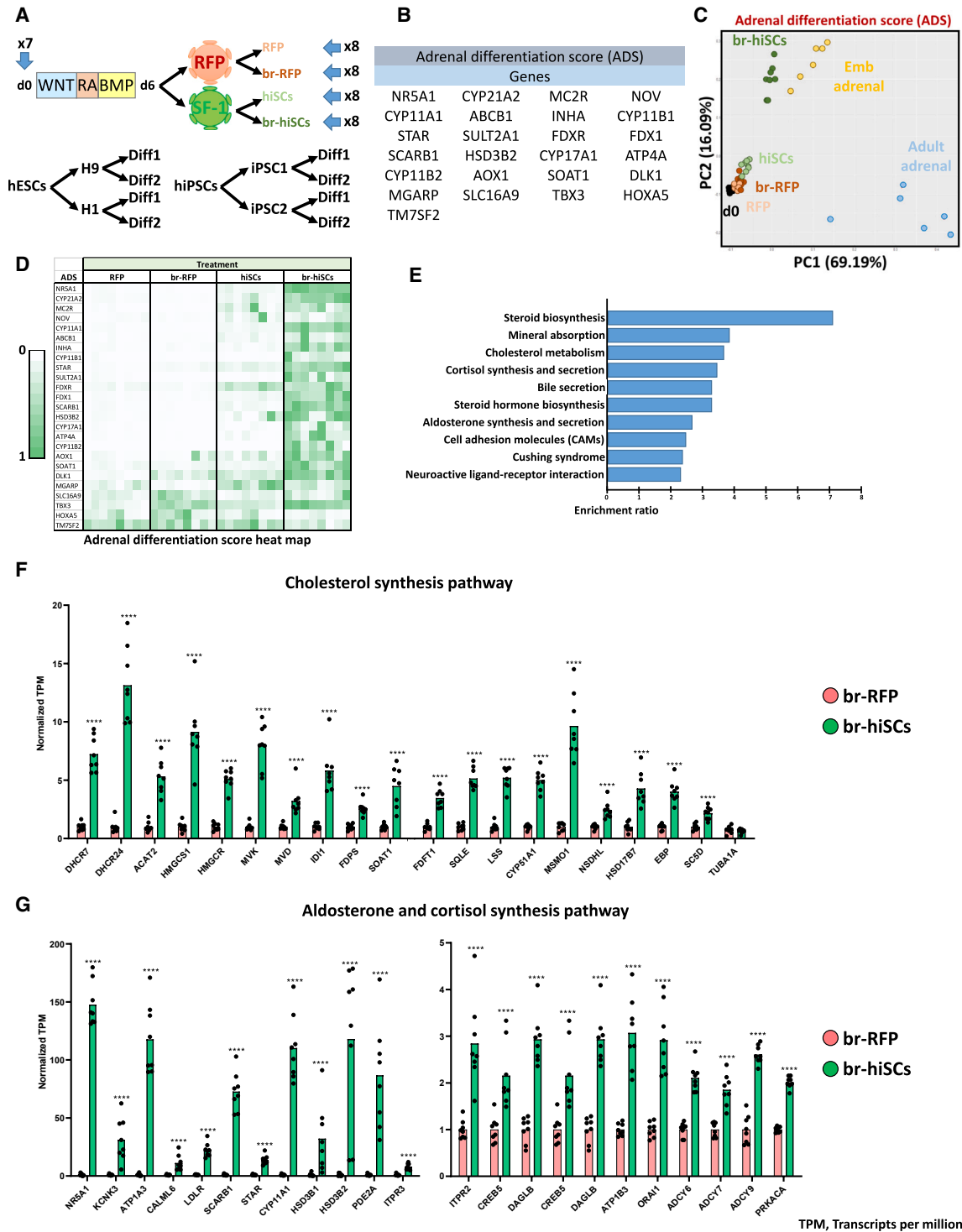
Figure 4. Bulk RNA-seq analysis of hiSCs

(A) Schematic of differentiation protocol with arrows indicating the number of samples collected for RNA-seq (top). Schematic of lines used and the number of differentiation conditions performed (lower).

(B) List of genes comprising the ADS.

(C) PCA of analyzed samples using the ADS gene set.

(D) Heatmap analysis of ADS genes in our differentiation system.

(legend continued on next page)

were subjected to bulk RNA sequencing (RNA-seq) analysis. To increase the robustness of the analysis, we employed two independent hESCs lines (H1 and H9) and two independent hiPSCs (iPSC1 and iPSC2). For each line, we performed two independent differentiation experiments (Figure 4A). We also analyzed the gene expression pattern of both embryonic and adult human adrenals. Principal component analysis (PCA) showed that gene expression profiles of undifferentiated cells differ significantly from those of differentiated cells, embryonic and adult adrenals (Figure S6A, left). Unlike pluripotent stem cells (filled black circles), all differentiated cell lines clustered closer to embryonic adrenal, consistent with the 6-day differentiation protocol directing cells toward an IM-like phenotype. Restricting the analysis only to differentiated cells, br-hiSCs showed a specific gene expression profile compared with RFP, br-RFP and hiSCs (Figure S6A, right). We then applied a previously established Adrenal Differentiation Score (ADS), based on a 25-gene signature[48] (Figure 4B). We focused the analysis on genes expressed in the adrenal cortex, and excluded genes expressed in the adrenal medulla, a separate tissue of neural crest origin not induced by our differentiation conditions. This analysis showed that br-hiSCs had an adrenocortical transcriptional pattern similar to embryonic adrenal, which is distinct from non-differentiated and differentiated cells without stimulation (Figures 4C and S6B). Heatmap analysis showed that most of the genes from the ADS are indeed upregulated in br-hiSCs (Figure 4D), as well as the steroidogenic enzymes required to synthesize hormones (Figure S6C). Over-representation analysis (ORA) of br-hiSCs compared with br-RFP (Figure 5E) shows a significant enrichment in genes related to steroid biosynthesis (Figure S6C), cholesterol metabolism (Figures 4F and S6D), and aldosterone and cortisol synthesis (Figure 4G). Interestingly, PCA analysis of all samples showed that the steroidogenic genetic program was achieved to a similar degree regardless of which cell type was used to differentiate the br-hiSCs or the time of differentiation (Figure S6E). Overall, these data show that expression of a steroidogenic genetic profile in br-hiSCs is highly reproducible among hiSC lines.

Single-cell adrenal signature comparison with br-hiSCs

Bulk RNA-seq demonstrates that br-hiSCs have a gene profile of immature adrenocortical cells. To further characterize the development stage of br-hiSCs, we took advantage of publicly available single-cell sequencing datasets from human adrenals at different stages of development, including fetal and neonatal time points. We pooled the single cell data from four adrenals at 8 weeks' gestation, from two different publications,[19,49] three adrenals at 12 weeks' gestation,[50] and two neonatal adrenals[50] (Figure 5A). Steroidogenic, endothelial, erythroid, immune, and mesenchymal cell populations were detected in all datasets (Figure 5B). In the fetal adrenals, we detected sub-populations of cells with an epithelial gene signature, chromaffin cells, Schwann

cell progenitor cells, and symphatoblasts.[49] All markers used for cluster identification are included in Table S1.

We next compared the significantly upregulated genes (log2 fold change ≥ 1 and p value ≤ 0.01) in br-hiSCs compared with br-RFP with the steroidogenic signature obtained from the single-cell steroidogenic cluster from both fetal and neonatal adrenals. We used the first 25 genes of each steroidogenic signature for comparison (a full list of genes in each signature can be found in Table S2). The fetal adrenal signature from the 12-week time point showed the highest percentage of genes upregulated in br-hiSCs (92%), followed by the 8-week time point (68%) and the neonatal time point (36%) (Figure 5C). Note that the probability of having a gene randomly upregulated in any given dataset was only 10.15% (2,594 genes upregulated from a total of 25,540 genes), which demonstrates that br-hiSCs are enriched in the steroidogenic signature. Moreover, PCA analysis of the bulk RNA-seq dataset, using the top 25 genes of the steroidogenic signatures, also show that br-hiSCs are closer in proximity to the 12-week fetal time point (Figure S7A).

As br-hiSCs most closely resemble the gene expression pattern of the 12-week fetal adrenal, we used this dataset for subsequent analyses. We used the steroidogenic cluster, defined by cells expressing steroidogenic enzymes such as *STAR*, *CYP11A1*, *CYP21A2*, *CYP17A1*, *CYP11B1*, and *CYP11B2*, and chromaffin cluster, defined by expression of *CHGA*, *CHGB*, *TH*, *DBH*, *STMN2*, and *CARTPT* (Figures 5D and S7B) to perform an enrichment analysis. For both the steroidogenic and chromaffin cells we used the first 200 genes defining the cluster. ORA show that only the combination of SF-1 and br-cAMP (br-hiSCs) results in an enrichment of steroidogenic profiles, while chromaffin gene expression is not enriched, used as a negative control (Figure 5E). Heat maps of the top 25 genes of steroidogenic and chromaffin signatures corroborate these results (Figure S7C). Taken together, these data demonstrate that br-hiSCs have a steroidogenic profile most closely related to the 12-week fetal adrenals.

Optimization of hormone production from hiSC lines

Next, we sought to identify strategies to optimize hormone production of hiSCs. First, we tested whether the addition of fetal bovine serum (FBS) might enhance steroidogenic potential. We exposed hiSCs to a range of serum concentrations in the presence or absence of br-cAMP. FBS significantly increase the steroidogenic potential of hiSCs in a dose-dependent manner (Figure 6A). Consistent with our previous data, addition of br-cAMP further enhances cortisol secreted into the medium.

We next assessed the ACTH responsiveness of hiSCs. From the bulk RNA-seq data we could detect an increase in MC2R (the ACTH receptor) and MRAP (the MC2R accessory protein) expression upon differentiation (Figure 6B). However, the level of both genes was notably lower than in human adrenal tissue (Figure S8A). Therefore, to increase ACTH responsiveness of

---

(E) ORA using the Kyoto Encyclopedia of Genes and Genomes tool from genes enriched in stimulated SF-1-expressing cells vs. stimulated mock-infected cells of significant genes with a p value of >0.05 and fold-change of >2.

(F) Representation of counts of genes involved in cholesterol synthesis between br-RFP and br-hiSCs.

(G) Representation of counts of gene involved in aldosterone and cortisol synthesis between br-RFP and br-hiSCs. All data are represented as mean ± SEM. TPM, transcripts per million. Statistical significance was determined using Student's t -est analysis between br-RFP and br-hiSCs for each gene. See also Figure S6.
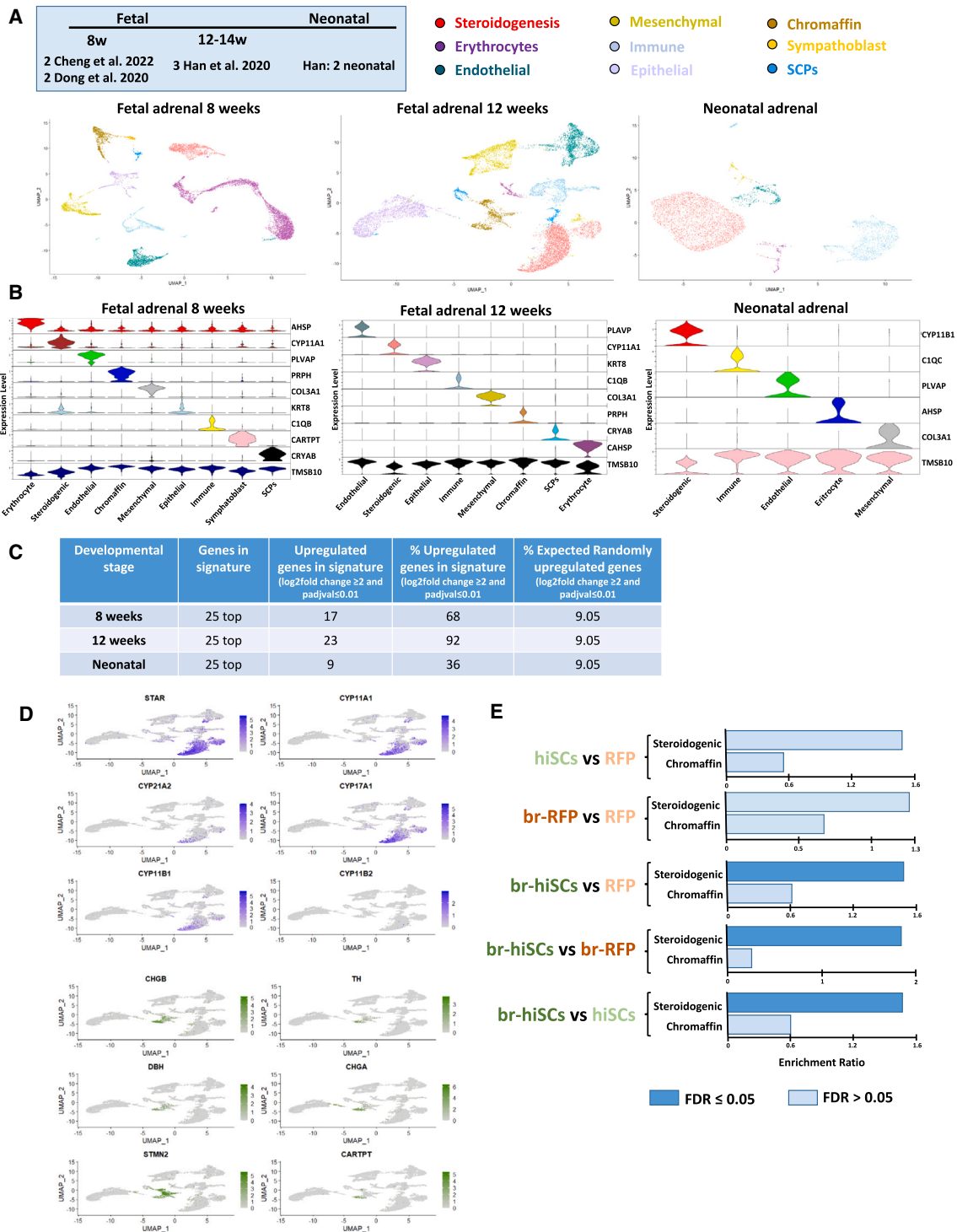
Figure 5. Comparison of differentially expressed genes between bulk RNA-seq and single cell adrenal signatures

(A) Uniform Manifold Approximation and Projection (UMAP) plots of four fetal adrenals at 8 weeks, three fetal adrenals at 12 weeks, and two neonatal adrenals. Nine clusters could be identified in the samples: Erythrocytes, sympathoblasts, Schwann cell precursors (SCPs), and steroidogenic, endothelial, mesenchymal, immune, epithelial and chromaffin cells.

(B) Violin plots of markers of each cell type.

(legend continued on next page)

hiSCs, we cloned a lentiviral vector to bicistronically express both MC2R and MRAP under the control of a the CMV promoter (Figure 6C). Differentiated cells were infected with a combination of SF-1 and MC2R/MRAP (hereafter called hiSCs-MM) and expression of transgenes and hormone secretion were assessed. RT-qPCR analysis revealed that all transgenes were expressed in each condition (Figure S8B). Immunocytochemistry (Figure 6D) corroborated MC2R, MRAP, and SF1 expression at the protein level. H295R, a human adrenocortical carcinoma cell line, was used as a positive control. hiSCs were able to secrete cortisol into the medium, but failed to respond to ACTH stimulation (Figure 6E). However, upon co-expression of SF-1, MC2R, and MRAP, hiSCs-MM cells responded to ACTH in a dose-dependent manner (Figure 6F), regardless of the cell of origin used. Taken together, these data suggest that the addition of serum to the protocol and the expression of MC2R/MRAP in hiSCs increase the cortisol production and their ACTH responsiveness, respectively.

An important advantage of hiSCs for potential cell therapies is their ability to proliferate while maintaining their steroidogenic potential (Figure S3E). To assess the capacity of hiSCs-MM to proliferate in the presence of ACTH, we performed double immunostaining using SF-1 and Ki67 (Figure 6G). Both basal and ACTH-stimulated hiSCs-MM have the ability to proliferate while retaining SF-1 expression, suggesting that hiSCs-MM can both proliferate and produce steroid hormones.

Disease modeling of triple A syndrome using hiPSCs-derived hiSCs

The derivation of hiPSCs combined with the rapid advances in precise DNA editing have dramatically accelerated the opportunity to study human diseases in the laboratory. To study the adrenal phenotype seen in patients with triple A syndrome, we used CRISPR-Cas9 to engineer a sub-clone of the hiPSC line KOLF2. We generated both a homozygous knock out of the *AAAS* gene (Figure S9A) and separately introduced one of the common mutations found in triple A syndrome, the splice-site mutation 43C>A in exon 1 (p.G14fs), which produces a frameshift resulting in a truncated ALADIN protein (protein product from the *AAAS* gene) (Figures S9B and S9C). We subjected wild-type (WT), knockout (KO), and G14fs lines to our differentiation protocol and generated four independent lines for each (Figure S9D). ALADIN protein was undetectable in KO and p.G14fs br-hiSCs by immunocytochemistry and western blot analysis, compared with WT br-hiSCs lines, while levels of SF-1 were similar (Figures 7A and 7B). In contrast, other nuclear pore complex proteins (recognized by the MAb414 antibody) were intact in all three lines (Figure S9E).

To assess the impact of AAAS loss on hormonal output in br-hiSCs, we analyzed cell culture supernatants by ELISA and LC-MS (Figure 7C). While all br-hiSCs secrete hormones, both the KO and G14fs lines secrete significantly lower levels cortisol, cortisone, corticosterone, and aldosterone than control lines (Fig-

ure 7C). In contrast, the steroidogenic intermediates upstream of cortisol and corticosterone are increased, especially in the KO lines, suggesting that the blockage occurred primarily at the level of 11β-hydroxylation (mediated by *CYP11B1* and *CYP11B2*). Indeed, the CYP11B1 enzyme is downregulated in the KO lines, assessed by western blot in three independent differentiations (Figure 7D). KO lines also showed reduced viability after two to three passages, compared with controls, possibly because of their inability to cope with stress and to progress through the cell cycle, as described in other KO models of AAAS.[26]

DISCUSSION

AI is characterized by adrenal hypofunction, with impaired secretion of glucocorticoids and, in some cases, mineralocorticoids and androgens. AI is a rare disease affecting 10–20 people per 100,000 population[1] that requires lifelong hormone replacement. Current hormone replacement strategies can lead to significant morbidity, including excess weight gain, hypertension, and the metabolic syndrome, along with under- or overtreatment in response to stress.[51] For these reasons, alternative therapies must be developed.

Cellular therapies using stem cells and reprogramming methods have recently emerged as potential solutions to treat diseases where endogenous cells and tissues do not function properly. In the adrenal field, such techniques have the potential to generate healthy and stress-responsive steroid-producing cells, leading to an alternative therapy for patients with AI. Although several groups have described the differentiation of steroid-producing cells from various cell sources,[52] no studies have provided proof that cells with adrenal characteristics can be expanded to the number required for cellular therapy while maintaining the ability to produce hormones after prolonged periods in culture. In most cases, cells terminally differentiate upon reprogramming.

Here, we report on a strategy to generate billions of hiSCs from a limited number of hPSCs. Our approach employs differentiation of hESCs or hiPSCs into adrenal precursor-like cells and subsequent expression of the transcription factor SF-1. Stem cell-derived differentiation protocols are subject to a high degree of variability among lines and between batches. To demonstrate the reproducibility of our protocol, we have generated hiSCs from two independent hESC lines and several hiPSC lines. At the gene expression level, differentiated hiSCs revealed a high degree of concordance. Moreover, hiSCs were consistently able to upregulate the steroidogenic machinery and secrete cortisol. Interestingly, hiSCs upregulate genes required for cholesterol biosynthesis, suggesting that, at least in part, the steroid hormones released by hiSCs are derived from *de novo* cholesterol synthesis. Importantly, the medium used to generate and expand hiSCs in our initial protocols was serum-free. However, the addition of serum to the medium increases the

---

(C) Number and percentage of upregulated genes in hiSCs compared with control+br-cAMP using the single-cell 25 top gene signatures of 8 weeks, 12 weeks, and neonatal adrenals.

(D) UMAP gene expression representation of steroidogenic (blue) and chromaffin (green) markers.

(E) Web Gestalt ORA of upregulated genes between conditions in the bulk RNA-seq using a 200-gene steroidogenic and medullary signature. See also Figure S7 and Tables S1 and S2.
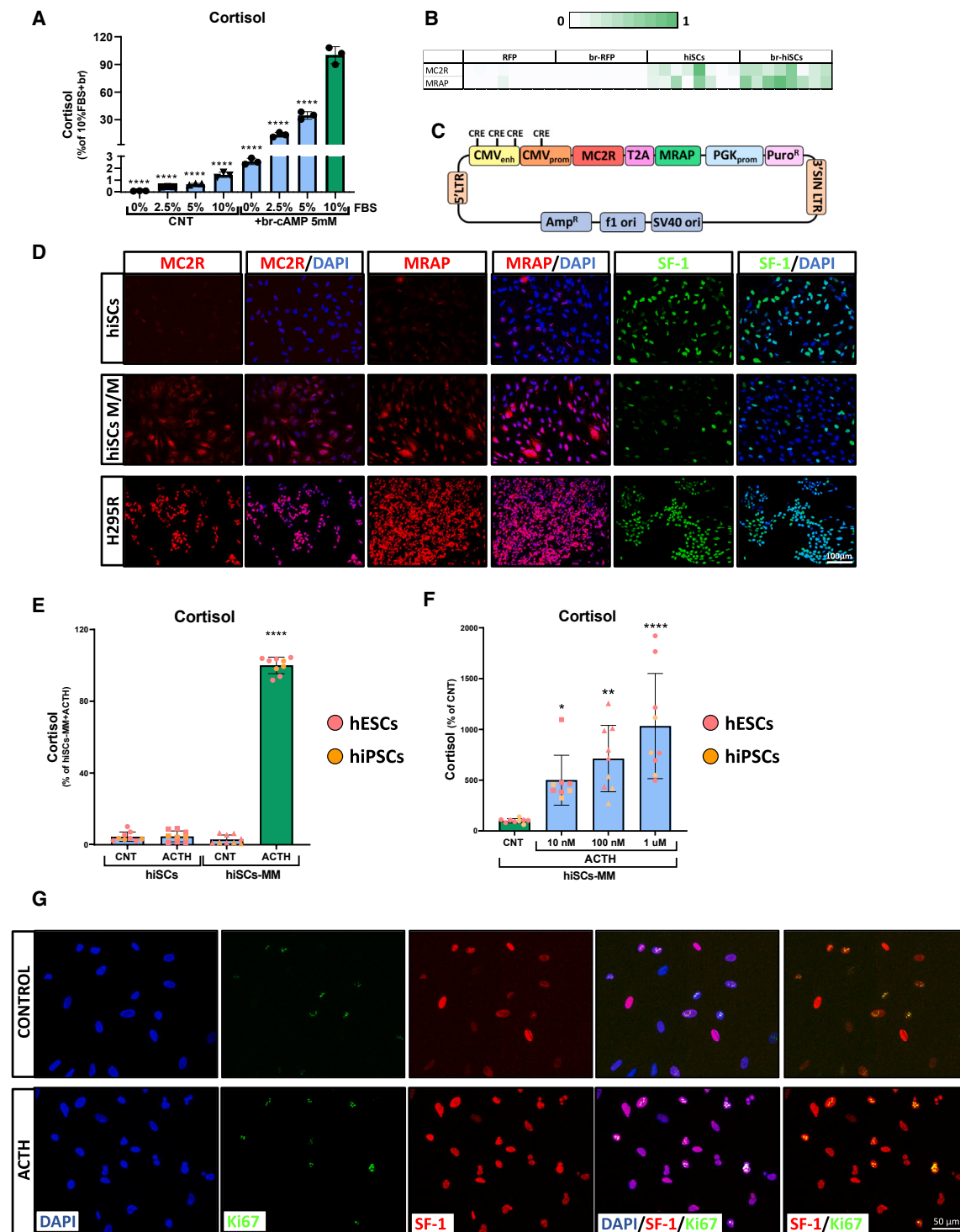
Figure 6. FBS and ACTH responsiveness of hiSCs

(A) Cortisol secretion in hiSCs after exposure to different concentrations of FBS for 48 h with or without 5 mM br-cAMP.

(B) Heatmap analysis of MC2R and MRAP expression from RNA-seq analysis.

(C) Schematic of the bicistronic vector used to co-express MC2R and MRAP under the CMV promoter in hiSCs.

(D) Immunocytochemistry of MC2R, MRAP and SF-1 in hiSCs, hiSCs-M/M, and H295R cells. Scale bar, 100 μm.

(E) Comparison of cortisol production analyzed by ELISA by vehicle or 1 μM ACTH between hiSCs and hiSCs-MM derived from hESCs or hiPSCs.

steroidogenic potential of the cells, possibly because of the greater abundance of cholesterol in the medium or unknown growth factors needed for steroidogenesis.

Several groups have recently published datasets of human adrenal glands at different stages of development.[49,50,53] Dong et al.[49] compared the genetic profile between neuroblastomas and early fetal adrenal development. Han et al.[50] analyzed, at a single cell level, all major human adult and fetal organs. Finally, Cheng et al.[53] focused their research on understanding the developmental origin and specification of the adrenal cortex in both humans and monkeys. Re-analyzing datasets from human fetal adrenals (from 8 to 12 weeks' gestation) and neonatal adrenals, we demonstrated that br-hiSCs share a steroidogenic signature most closely related to human fetal adrenals at 12 weeks' gestation. It is not unusual in differentiation protocols using pluripotent stem cells to obtain fetal-like cells; in other endocrine differentiation systems, like the generation of pancreatic beta-cells from hPSCs, comparison between differentiated cell types produced *in vitro* and their *in vivo* counterparts show that hPSC-derived beta cells more closely resemble human fetal beta cells than adult beta cells.[54] Similar outcomes can be seen in the production of red blood cells,[55] inner ear cells,[56] intestinal tissue,[57] microglia,[58] and cardiomyocytes.[59]

Recently, Sakata et al.[16] elegantly demonstrated the ability to generate human fetal zone adrenal-cortex-like cells from hPSCs. Similar to our protocol, the authors used morphogens such as WNT, RA, and BMP4 for the initial steps of differentiation. In contrast to our protocol, Sakata et al. cultivated cells in a 3D matrix (extracellular matrix) from the beginning of their protocol. Interestingly, initial attempts using this combination of small molecules, like in our protocol, did not activate NR5A1. Of note, incorporation of 10% KO serum replacement together with NODAL/Activin inhibitors, NOTCH inhibitors, SHH signaling and, at a later stage, WNT inhibition, lead to detectable expression of NR5A1. In their differentiation protocol, cells produce Δ5 steroids such as dehydroepiandrosterone and dehydroepiandrosterone sulfate, while Δ4 steroid production (i.e., cortisol, aldosterone) was undetectable, consistent with a fetal adrenal phenotype. In contrast, hiSCs produce adult Δ4 steroids, possibly because of a direct effect of higher levels of SF-1 expression to promote steroidogenesis. Importantly, cortisol and its precursors are detected in human fetal adrenals as early as 12 weeks.[60] Studying pathways and the sub-set of genes upregulated from the transition of fetal to adult tissue from the single cell datasets will shed light on potential mechanisms required to promote maturation of differentiated cells, becoming a powerful tool to improve differentiation protocols in the future.

We previously used differentiated steroidogenic cells from patients with CAH, resulting from CYP21A2 deficiency, to model this disease *in vitro*,[6] demonstrating that gene therapy could be an option for these patients to restore normal steroidogenesis. This approach to treat CAH has also been tested *in vivo*[61] and is currently undergoing clinical trials (ClinicalTrials.gov Identifier: NCT04783181) using an AAV5 virus.[62] We harnessed the potential of stem cell-derived steroidogenic cells to model

another adrenal disease, the triple A syndrome, which includes glucocorticoid deficiency in up to 85% of patients.[63]

Triple A syndrome results from mutations in *AAAS*, encoding the 546-aa protein ALADIN. ALADIN consists of seven WD (tryptophan-aspartic acid) repeats, which serve as a rigid scaffold or platform for reversible protein-protein interactions and protein complex assemblies.[64] ALADIN is expressed ubiquitously in human tissues and is particularly abundantly in the adrenal gland, gastrointestinal tissues, pituitary gland, and cerebellum,[64,65] which probably explains the main AAAS manifestations. ALADIN is one of the nucleoporins from the nuclear pore complex (NPC), a multiprotein structure spanning the double nuclear membrane involved in nucleocytoplasmic exchange.[66] In most cases, ALADIN mutations lead to mistargeting of the protein in the NPC, impairing nuclear import of proteins involved in DNA-repair such as aprataxin and DNA ligase, or the antioxidant protein ferritin heavy chain, leading to oxidative stress.[67,68]

We engineered an iPSC line using CRISPR-Cas9 to knock out *AAAS* and generated br-hiSCs. We can detect a reduction of steroidogenesis, with lower levels of glucocorticoid and mineralocorticoid secretion compared with its isogeneic control line. These results are consistent with the phenotype seen in triple A patients, where cortisol levels,[69] and in some cases aldosterone levels,[70] are reduced. Interestingly, we detect a block in steroidogenesis at the level of 11β-hydroxylation, mediated by CYP11B1 in the zona fasciculata (to convert 11-deoxycortisol to cortisol) and CYP11B2 in the zona glomerulosa (to convert 11-deoxycorticosterone to corticosterone). Western blot analysis of CYP11B1 demonstrates a downregulation of the enzyme in KO lines. Future research should focus on studying potential interactions between ALADIN and 11β-hydroxylation and the mechanisms leading to impaired steroidogenesis.

Also of interest, hiSCs KO lines showed impaired proliferation and degenerate after two or three passages. This observation is not entirely surprising, as loss of ALADIN leads to oxidative stress in the cells.[26] Steroidogenic cells have an increased mitochondrial activity (where key steps in steroidogenesis take place) and have high levels of reactive oxygen species, a byproduct of the respiratory chain, which have deleterious effects on proteins, lipids, and nucleic acids, and subsequently lead to cellular dysfunction and death. Indeed, adrenals of patients with triple A syndrome demonstrate adrenal atrophy.[24]

A similar, albeit milder, impairment in steroidogenesis was shown using an iPSCs line harboring a common ALADIN mutation found in triple A patients, G14fs (43C>A).[25] Interestingly, initial overexpression experiments using this ALADIN mutation showed that the protein remains in the nuclear pore.[71] Detailed analysis of this mutation using fibroblast lines from a heterozygous patient revealed that the mutation causes a frameshift due to a novel splice donor site, resulting in a shortened protein due to a premature stop codon. These results are consistent with our immunofluorescent and western blot analyses, where we were unable to detect the protein in our mutant lines, using an antibody that detects the

F) Cortisol production analyzed by ELISA of hiSCs-MM derived from hESCs or hiPSCs upon ACTH stimulation or without (CNT).

(G) Immunocytochemistry of Ki67 (green) and SF-1 (red) in hiSCs-MM untreated and treated with 1 μM ACTH for 24 h. Scale bar, 50 μm. All data are represented as mean ± SEM. Green bars depict the column used for comparison to other bars. Statistical significance was determined using one-way ANOVA followed by Dunnet's multiple comparison test correction. See also Figure S8.
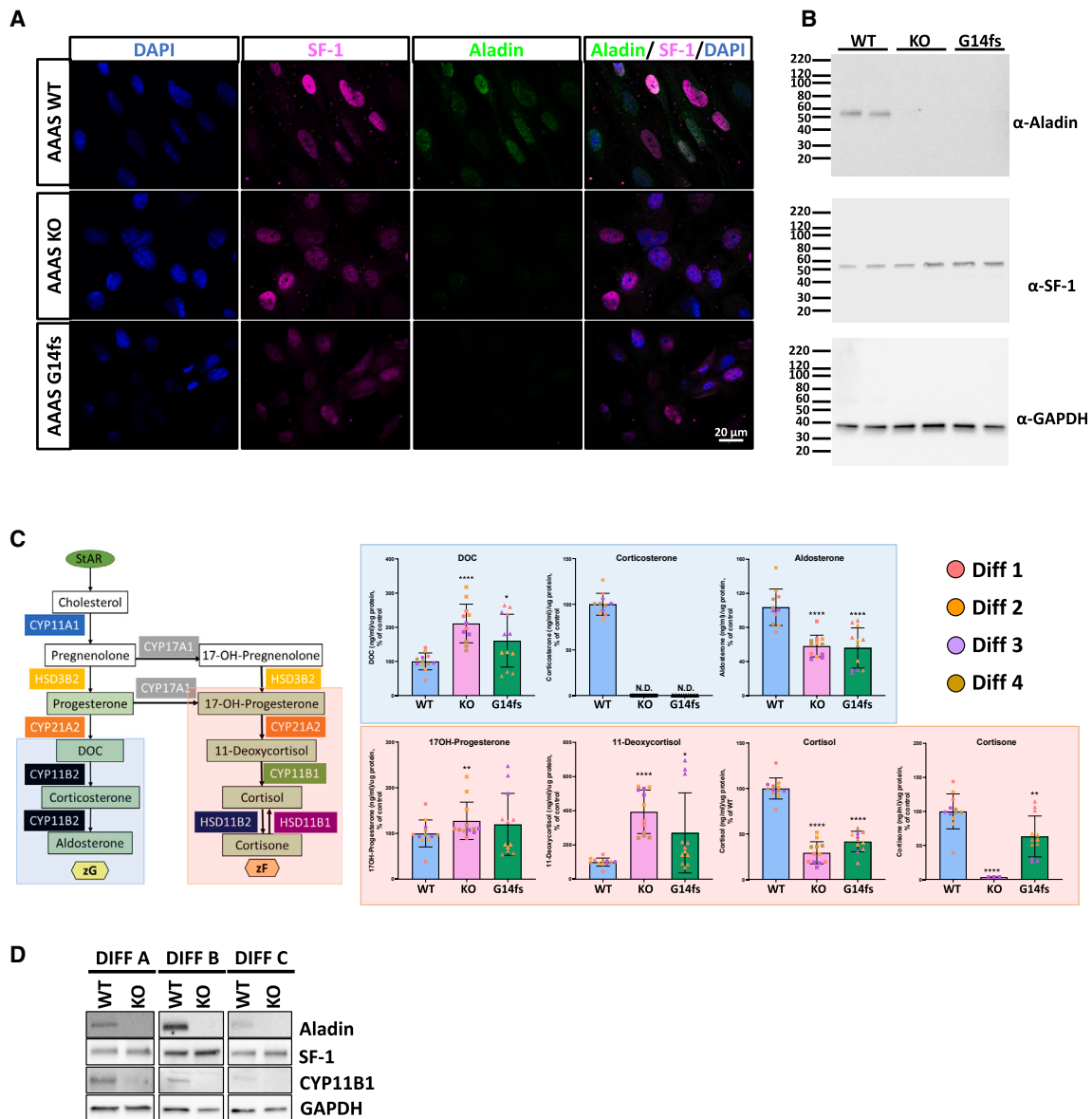
Figure 7. Modeling triple A syndrome using hiSCs

(A) Immunocytochemistry for ALADIN (green) and SF-1 (magenta) in WT, KO, and G14fs human hiSCs cell lines. DAPI (in blue) indicates nuclear staining. Scale bar, 20 μm.

(B) Western blot analysis for Aladin, SF-1, and GAPDH of WT, KO, and G14fs human br-hiSCs cell lines.

(C) Secretion of adrenal steroids from WT, KO, and G14fs human hiSC lines assessed by ELISA or mass spectrometry. (Left) Representation of steroidogenic pathway in the adrenal gland. Statistical significance was determined using one-way ANOVA followed by Dunnet's multiple comparison test correction, comparing the WT lines with KO and G14fs lines.

(D) Western blot analysis of WT and kO hiSCs using Aladin, SF-1, CYP11B1, and GAPDH antibodies. All data are represented as mean ± SEM. See also Figure S9.

C-terminal end of ALADIN. A shortened protein containing the N-terminal domain may explain why hiSCs harboring the G14fs mutation do not show the extreme phenotype seen in hiSCs null for AAAS. As mouse models of triple A syndrome do not recapitulate the human disease[25] and in vitro overexpression experiments using fibroblast are misleading,[71] hiSCs derived from patient-specific iPSCs seem to more closely recapitulate the human disease.

In summary, using the serial addition of WNT, RA, and BMP4, followed by SF-1 expression and PKA activation, we report on the directed differentiation of hPSCs into hiSCs that resemble fetal adrenal cells capable of dramatic expansion and production of cortisol. Moreover, this protocol enabled modeling of the AI resulting from loss-of-function mutations in AAAS, providing new mechanistic insight into the triple A syndrome. To further refine the conditions necessary to generate clinical grade adrenal cells

CellPress
OPEN ACCESS

suitable for transplantation in patients with AI, future efforts should focus on strategies to encapsulate hiSCs followed by validation using models of AI, *in vivo*.

Limitations of the study

The generation of CRISPR-Cas9-modified cell lines may result in undesired phenotypes caused by potential off-target genetic alterations. Further application of the editing approaches we report here will require comprehensive DNA sequencing of the generated cell lines to avoid introducing unintended changes that could result in oncogenic transformation or off-target phenotypes. We have not undertaken such sequencing here. Potential strategies to mitigate oncogenic risk include integrating suicide genes into the cell lines and encapsulating them within retrievable, bioengineered devices. Such devices also hold promise for avoiding immune rejection of human leukocyte antigen-non-identical cells. Another important avenue for further development and application of the cells we generate in this study is to assess the ability of engrafted cells to produce physiological levels of hormone *in vivo*, which we also have not undertaken here.

STAR★METHODS

Detailed methods are provided in the online version of this paper and include the following:

- KEY RESOURCES TABLE
- RESOURCE AVAILABILITY
  - Lead contact
  - Materials availability
  - Data and code availability
- EXPERIMENTAL MODEL AND STUDY PARTICIPANT DETAILS
  - Cell culture
  - Cell lines
  - Human samples
- METHOD DETAILS
  - Antibodies
  - Generation of CRISPR-Cas9 genome engineered lines
  - Generation of pLJM1-MC2R-MRAP-Puro vector
  - Lentivirus production
  - Cell differentiation
  - Immunocytochemistry
  - Immunohistochemistry
  - Gene expression analysis
  - Hormone quantification
  - ELISA
  - LC-MS/MS procedure
  - Transmission electron microscopy
  - Bioinformatic analysis
  - Bulk matrix of counts
  - Pseudobulking and bulk clustering analysis
  - Nile Red Staining
  - WB analysis
  - Data analysis
- QUANTIFICATION AND STATISTICAL ANALYSIS

AUTHOR CONTRIBUTIONS

G.R.B. designed the research, conducted experiments, acquired and analyzed data, and wrote the manuscript; A.E., M.M., and K.B. conducted experiments and acquired and analyzed data; F.A.J. analyzed bulk and single-cell sequencing data; T.M. and R.M. provided and gave advice on hESCs cell lines; S.Q. and W.C.S. generated the AAAS cell lines; A.R.D.C., J.P.C., and H.L.S. provided the AAAS cell lines; L.G. helped to design the experiments; D.L.C., B.L., and L.G. revised the manuscript; and D.T.B. and S.R.B. supervised the research, helped to design the experiments, and wrote the manuscript.

DECLARATION OF INTERESTS

G.R.B. and S.R.B. have filed the patent application WO2023/083839 A1.

INCLUSION AND DIVERSITY

We support inclusive, diverse, and equitable conduct of research.

REFERENCES

1. Hahner, S., Ross, R.J., Arlt, W., Bancos, I., Burger-Stritt, S., Torpy, D.J., Husebye, E.S., and Quinkler, M. (2021). Adrenal insufficiency. Nat. Rev. Dis. Prim. *7*, 19–24. https://doi.org/10.1038/S41572-021-00252-7.

2. Huang, H., Zou, X., Zhong, L., Hou, Y., Zhou, J., Zhang, Z., Xing, X., and Sun, J. (2019). CRISPR/dCas9-mediated activation of multiple endogenous target genes directly converts human foreskin fibroblasts into Leydig-like cells. J. Cell Mol. Med. *23*, 6072–6084. https://doi.org/10.1111/JCMM.14470.

3. Yang, Y., Li, Z., Wu, X., Chen, H., Xu, W., Xiang, Q., Zhang, Q., Chen, J., Ge, R.-S., Su, Z., and Huang, Y. (2017). Stem Cell Reports Article Direct Reprogramming of Mouse Fibroblasts toward Leydig-like Cells by Defined Factors. Stem Cell Rep. *8*, 39–53. https://doi.org/10.1016/j.stemcr.2016.11.010.

4. Gondo, S., Yanase, T., Okabe, T., Tanaka, T., Morinaga, H., Nomura, M., Goto, K., and Nawata, H. (2004). SF-1/Ad4BP transforms primary long-term cultured bone marrow cells into ACTH-responsive steroidogenic

cells. Gene Cell. *9*, 1239–1247. https://doi.org/10.1111/j.1365-2443.2004.00801.x.

5. Gondo, S., Okabe, T., Tanaka, T., Morinaga, H., Nomura, M., Takayanagi, R., Nawata, H., and Yanase, T. (2008). Adipose tissue-derived and bone marrow-derived mesenchymal cells develop into different lineage of steroidogenic cells by forced expression of steroidogenic factor 1. Endocrinology *149*, 4717–4725. https://doi.org/10.1210/en.2007-1808.

6. Ruiz-Babot, G., Balyura, M., Hadjidemetriou, I., Ajodha, S.J., Taylor, D.R., Ghataore, L., Taylor, N.F., Schubert, U., Ziegler, C.G., Storr, H.L., et al. (2018). Modeling Congenital Adrenal Hyperplasia and Testing Interventions for Adrenal Insufficiency Using Donor-Specific Reprogrammed Cells. Cell Rep. *22*, 1236–1249. https://doi.org/10.1016/j.celrep.2018.01.003.

7. Tanaka, T., Aoyagi, C., Mukai, K., Nishimoto, K., Kodama, S., and Yanase, T. (2020). Extension of Survival in Bilaterally Adrenalectomized Mice by Implantation of SF-1/Ad4BP-Induced Steroidogenic Cells. Endocrinology *161*, bqaa007. https://doi.org/10.1210/ENDOCR/BQAA007.

8. Tanaka, T., Gondo, S., Okabe, T., Ohe, K., Shirohzu, H., Morinaga, H., Nomura, M., Tani, K., Takayanagi, R., Nawata, H., and Yanase, T. (2007). Steroidogenic factor 1/adrenal 4 binding protein transforms human bone marrow mesenchymal cells into steroidogenic cells. J. Mol. Endocrinol. *39*, 343–350. https://doi.org/10.1677/JME-07-0076.

9. Wei, X., Peng, G., Zheng, S., and Wu, X. (2012). Differentiation of umbilical cord mesenchymal stem cells into steroidogenic cells in comparison to bone marrow mesenchymal stem cells. Cell Prolif. *45*, 101–110. https://doi.org/10.1111/j.1365-2184.2012.00809.x.

10. Yazawa, T., Inanoka, Y., Mizutani, T., Kuribayashi, M., Umezawa, A., and Miyamoto, K. (2009). Liver receptor homolog-1 regulates the transcription of steroidogenic enzymes and induces the differentiation of mesenchymal stem cells into steroidogenic cells. Endocrinology *150*, 3885–3893. https://doi.org/10.1210/en.2008-1310.

11. Yazawa, T., Mizutani, T., Yamada, K., Kawata, H., Sekiguchi, T., Yoshino, M., Kajitani, T., Shou, Z., Umezawa, A., and Miyamoto, K. (2006). Differentiation of adult stem cells derived from bone marrow stroma into Leydig or adrenocortical cells. Endocrinology *147*, 4104–4111. https://doi.org/10.1210/en.2006-0162.

12. Yazawa, T., Kawabe, S., Inaoka, Y., Okada, R., Mizutani, T., Imamichi, Y., Ju, Y., Yamazaki, Y., Usami, Y., Kuribayashi, M., et al. (2011). Differentiation of mesenchymal stem cells and embryonic stem cells into steroidogenic cells using steroidogenic factor-1 and liver receptor homolog-1. Mol. Cell. Endocrinol. *336*, 127–132. https://doi.org/10.1016/j.mce.2010.11.025.

13. Crawford, P.A., Sadovsky, Y., and Milbrandt, J. (1997). Nuclear receptor steroidogenic factor 1 directs embryonic stem cells toward the steroidogenic lineage. Mol. Cell Biol. *17*, 3997–4006.

14. Jadhav, U., and Jameson, J.L. (2011). Steroidogenic factor-1 (SF-1)-driven differentiation of murine embryonic stem (ES) cells into a gonadal lineage. Endocrinology *152*, 2870–2882. https://doi.org/10.1210/en.2011-0219.

15. Sonoyama, T., Sone, M., Honda, K., Taura, D., Kojima, K., Inuzuka, M., Kanamoto, N., Tamura, N., and Nakao, K. (2012). Differentiation of human embryonic stem cells and human induced pluripotent stem cells into steroid-producing cells. Endocrinology *153*, 4336–4345. https://doi.org/10.1210/en.2012-1060.

16. Sakata, Y., Cheng, K., Mayama, M., Seita, Y., Detlefsen, A.J., Mesaros, C.A., Penning, T.M., Shishikura, K., Yang, W., Auchus, R.J., et al. (2022). Reconstitution of human adrenocortical specification and steroidogenesis using induced pluripotent stem cells. Dev. Cell *57*, 2566–2583.e8. https://doi.org/10.1016/J.DEVCEL.2022.10.010.

17. Li, L., Li, Y., Sottas, C., Culty, M., Fan, J., Hu, Y., Cheung, G., Chemes, H.E., and Papadopoulos, V. (2019). Directing differentiation of human induced pluripotent stem cells toward androgen-producing Leydig cells rather than adrenal cells. Proc. Natl. Acad. Sci. USA *116*, 23274–23283. https://doi.org/10.1073/PNAS.1908207116/-/DCSUPPLEMENTAL.

18. Takasato, M., and Little, M.H. (2015). The origin of the mammalian kidney: implications for recreating the kidney in vitro. Development *142*, 1937–1947, –1947. https://doi.org/10.1242/DEV.104802.

19. Cheng, K., Seita, Y., Moriwaki, T., Noshiro, K., Sakata, Y., Hwang, Y.S., Torigoe, T., Saitou, M., Tsuchiya, H., Iwatani, C., et al. (2022). The developmental origin and the specification of the adrenal cortex in humans and cynomolgus monkeys. Sci. Adv. *8*, 8485. https://doi.org/10.1126/SCIADV.ABN8485/SUPPL_FILE/SCIADV.ABN8485_TABLES_-S1_TO_S6.ZIP.

20. Duester, G. (2008). Retinoic acid synthesis and signaling during early organogenesis. Cell *134*, 921–931. https://doi.org/10.1016/J.CELL.2008.09.002.

21. Dihazi, G.H., Mueller, G.A., Asif, A.R., Eltoweissy, M., Wessels, J.T., and Dihazi, H. (2015). Proteomic characterization of adrenal gland embryonic development reveals early initiation of steroid metabolism and reduction of the retinoic acid pathway. Proteome Sci. *13*, 6–14. https://doi.org/10.1186/S12953-015-0063-8/FIGURES/7.

22. James, R.G., and Schultheiss, T.M. (2005). Bmp signaling promotes intermediate mesoderm gene expression in a dose-dependent, cell-autonomous and translation-dependent manner. Dev. Biol. *288*, 113–125. https://doi.org/10.1016/J.YDBIO.2005.09.025.

23. Araoka, T., Mae, S.I., Kurose, Y., Uesugi, M., Ohta, A., Yamanaka, S., and Osafune, K. (2014). Efficient and Rapid Induction of Human iPSCs/ESCs into Nephrogenic Intermediate Mesoderm Using Small Molecule-Based Differentiation Methods. PLoS One *9*, 84881. https://doi.org/10.1371/JOURNAL.PONE.0084881.

24. Allgrove, J., Clayden, G.S., Grant, D.B., and Macaulay, J.C. (1978). Familial glucocorticoid deficiency with achalasia of the cardia and deficient tear production. Lancet *1*, 1284–1286. https://doi.org/10.1016/S0140-6736(78)91268-0.

25. Huebner, A., Kaindl, A.M., Knobeloch, K.P., Petzold, H., Mann, P., and Koehler, K. (2004). The triple A syndrome is due to mutations in ALADIN, a novel member of the nuclear pore complex. Endocr. Res. *30*, 891–899. https://doi.org/10.1081/ERC-200044138.

26. Prasad, R., Metherell, L.A., Clark, A.J., and Storr, H.L. (2013). Deficiency of ALADIN impairs redox homeostasis in human adrenal cells and inhibits steroidogenesis. Endocrinology *154*, 3209–3218. https://doi.org/10.1210/EN.2013-1241.

27. Huebner, A., Mann, P., Rohde, E., Kaindl, A.M., Witt, M., Verkade, P., Jakubiczka, S., Menschikowski, M., Stoltenburg-Didinger, G., and Koehler, K. (2006). Mice lacking the nuclear pore complex protein ALADIN show female infertility but fail to develop a phenotype resembling human triple A syndrome. Mol. Cell Biol. *26*, 1879–1887. https://doi.org/10.1128/MCB.26.5.1879-1887.2006.

28. Luo, X., Ikeda, Y., and Parker, K.L. (1994). A cell-specific nuclear receptor is essential for adrenal and gonadal development and sexual differentiation. Cell *77*, 481–490. https://doi.org/10.1016/0092-8674(94)90211-9.

29. Zanaria, E., Muscatelli, F., Bardoni, B., Strom, T.M., Guioli, S., Guo, W., Lalli, E., Moser, C., Walker, A.P., McCabe, E.R., et al. (1994). An unusual member of the nuclear hormone receptor superfamily responsible for X-linked adrenal hypoplasia congenita. Nature *372*, 635–641. https://doi.org/10.1038/372635A0.

30. Bandiera, R., Vidal, V.P.I., Motamedi, F.J., Clarkson, M., Sahut-Barnola, I., VonGise, A., Pu, W.T., Hohenstein, P., Martinez, A., and Schedl, A. (2013). WT1 Maintains Adrenal-Gonadal Primordium Identity and Marks a Population of AGP-like Progenitors within the Adrenal Gland. Dev. Cell *27*, 5–18. https://doi.org/10.1016/j.devcel.2013.09.003.

31. Ketola, I., Pentikäinen, V., Vaskivuo, T., Ilvesmäki, V., Herva, R., Dunkel, L., Tapanainen, J.S., Toppari, J., and Heikinheimo, M. (2000). Expression of Transcription Factor GATA-4 during Human Testicular Development and Disease. J. Clin. Endocrinol. Metab. *85*, 3925–3931. https://doi.org/10.1210/JCEM.85.10.6900.

32. Tevosian, S.G., Jiménez, E., Hatch, H.M., Jiang, T., Morse, D.A., Fox, S.C., and Padua, M.B. (2015). Adrenal development in mice requires GATA4 and GATA6 transcription factors. Endocrinology *156*, 2503–2517. https://doi.org/10.1210/en.2014-1815.

33. Garcia-Alonso, L., Lorenzi, V., Mazzeo, C.I., Alves-Lopes, J.P., Roberts, K., Sancho-Serra, C., Engelbert, J., Marečková, M., Gruhn, W.H., Botting, R.A., et al. (2022). Single-cell roadmap of human gonadal development. Nature *607*, 540–547. https://doi.org/10.1038/S41586-022-04918-4.

34. Bouchard, M., Souabni, A., Mandler, M., Neubüser, A., and Busslinger, M. (2002). Nephric Lineage Specification by Pax2 and Pax8. https://doi.org/10.1101/gad.240102.

35. Hadjidemetriou, I., Mariniello, K., Ruiz-Babot, G., Pittaway, J., Mancini, A., Mariannis, D., Gomez-Sanchez, C.E., Parvanta, L., Drake, W.M., Chung, T.-T., et al. (2019). DLK1/PREF1 marks a novel cell population in the human adrenal cortex. J. Steroid Biochem. Mol. Biol. *193*, 105422. https://doi.org/10.1016/j.jsbmb.2019.105422.

36. Liu, P., Wakamiya, M., Shea, M.J., Albrecht, U., Behringer, R.R., and Bradley, A. (1999). Requirement for Wnt3 in vertebrate axis formation. Nat. Genet. *22*, 361–365. https://doi.org/10.1038/11932.

37. Huelsken, J., Vogel, R., Brinkmann, V., Erdmann, B., Birchmeier, C., and Birchmeier, W. (2000). Requirement for beta-catenin in anterior-posterior axis formation in mice. J. Cell Biol *148*, 567–578, 2000 Feb 7. https://doi.org/10.1083/jcb.148.3.567.

38. Lindsley, R.C., Gill, J.G., Kyba, M., Murphy, T.L., and Murphy, K.M. (2006). Canonical Wnt signaling is required for development of embryonic stem cell-derived mesoderm. Development *133*, 3787–3796. https://doi.org/10.1242/DEV.02551.

39. Takasato, M., Er, P.X., Chiu, H.S., Maier, B., Baillie, G.J., Ferguson, C., Parton, R.G., Wolvetang, E.J., Roost, M.S., Chuva de Sousa Lopes, S.M., and Little, M.H. (2015). Kidney organoids from human iPS cells contain multiple lineages and model human nephrogenesis. Nature *526*, 564–568. https://doi.org/10.1038/nature15695.

40. Zubair, M., Ishihara, S., Oka, S., Okumura, K., and Morohashi, K. -i. (2006). Two-Step Regulation of Ad4BP/SF-1 Gene Transcription during Fetal Adrenal Development: Initiation by a Hox-Pbx1-Prep1 Complex and Maintenance via Autoregulation by Ad4BP/SF-1. Mol. Cell Biol. *26*, 4111–4121. https://doi.org/10.1128/MCB.00222-06.

41. Mugford, J.W., Sipilä, P., McMahon, J.A., and McMahon, A.P. (2008). Osr1 expression demarcates a multi-potent population of intermediate mesoderm that undergoes progressive restriction to an Osr1-dependent nephron progenitor compartment within the mammalian kidney. Dev. Biol. *324*, 88–98. https://doi.org/10.1016/J.YDBIO.2008.09.010.

42. Yang, Y., Workman, S., and Wilson, M.J. (2019). The molecular pathways underlying early gonadal development. J. Mol. Endocrinol. *62*, R47–R64. https://doi.org/10.1530/JME-17-0314.

43. Moore, A.W., McInnes, L., Kreidberg, J., Hastie, N.D., and Schedl, A. (1999). YAC complementation shows a requirement for Wt1 in the development of epicardium, adrenal gland and throughout nephrogenesis. Development *126*, 1845–1857.

44. Miller, W.L., and Bose, H.S. (2011). Early steps in steroidogenesis: intracellular cholesterol trafficking: Thematic Review Series: Genetics of Human Lipid Diseases. J. Lipid Res. *52*, 2111–2135. https://doi.org/10.1194/JLR.R016675.

45. Wang, X.L., Bassett, M., Zhang, Y., Yin, S., Clyne, C., White, P.C., and Rainey, W.E. (2000). Transcriptional regulation of human 11beta-hydroxylase (hCYP11B1). Endocrinology *141*, 3587–3594. https://doi.org/10.1210/ENDO.141.10.7689.

46. Rodriguez, H., Hum, D.W., Staels, B., and Miller, W.L. (1997). Transcription of the Human Genes for Cytochrome P450scc and P450c17 Is Regulated Differently in Human Adrenal NCI-H295 Cells Than in Mouse Adrenal Y1 Cells. J. Clin. Endocrinol. Metab. *82*, 365–371. https://doi.org/10.1210/JCEM.82.2.3721.

47. Fickenscher, H., Stamminger, T., Rüger, R., and Fleckenstein, B. (1989). The role of a repetitive palindromic sequence element in the human cytomegalovirus major immediate early enhancer. J. Gen. Virol. *70*, 107–123, Pt 1. https://doi.org/10.1099/0022-1317-70-1-107/CITE/REFWORKS.

48. Zheng, S., Cherniack, A.D., Dewal, N., Moffitt, R.A., Danilova, L., Murray, B.A., Lerario, A.M., Else, T., Knijnenburg, T.A., Ciriello, G., et al. (2016). Comprehensive Pan-Genomic Characterization of Adrenocortical Carcinoma. Cancer Cell *29*, 723–736. https://doi.org/10.1016/J.CCELL.2016.04.002.

49. Dong, R., Yang, R., Zhan, Y., Lai, H.D., Ye, C.J., Yao, X.Y., Luo, W.Q., Cheng, X.M., Miao, J.J., Wang, J.F., et al. (2020). Single-Cell Characterization of Malignant Phenotypes and Developmental Trajectories of Adrenal Neuroblastoma. Cancer Cell *38*, 716–733.e6. https://doi.org/10.1016/J.CCELL.2020.08.014.

50. Han, X., Zhou, Z., Fei, L., Sun, H., Wang, R., Chen, Y., Chen, H., Wang, J., Tang, H., Ge, W., et al. (2020). Construction of a human cell landscape at single-cell level. Nature *581*, 303–309. https://doi.org/10.1038/s41586-020-2157-4.

51. Giordano, R., Marzotti, S., Balbo, M., Romagnoli, S., Marinazzo, E., Berardelli, R., Migliaretti, G., Benso, A., Falorni, A., Ghigo, E., and Arvat, E. (2009). Metabolic and cardiovascular profile in patients with Addison's disease under conventional glucocorticoid replacement. J. Endocrinol. Invest. *32*, 917–923. https://doi.org/10.1007/BF03345773.

52. Ruiz-Babot, G., Hadjidemetriou, I., King, P.J., and Guasti, L. (2015). New directions for the treatment of adrenal insufficiency. Front. Endocrinol. *6*, 70–78. https://doi.org/10.3389/fendo.2015.00070.

53. Cheng, K., Seita, Y., Moriwaki, T., Noshiro, K., Sakata, Y., Hwang, Y.S., Torigoe, T., Saitou, M., Tsuchiya, H., Iwatani, C., et al. (2022). The developmental origin and the specification of the adrenal cortex in humans and cynomolgus monkeys. Sci. Adv. *8*, eabn8485. https://doi.org/10.1126/SCIADV.ABN8485.

54. Hrvatin, S., O'Donnell, C.W., Deng, F., Millman, J.R., Pagliuca, F.W., DiIorio, P., Rezania, A., Gifford, D.K., and Melton, D.A. (2014). Differentiated human stem cells resemble fetal, not adult, β cells. Proc. Natl. Acad. Sci. USA *111*, 3038–3043. https://doi.org/10.1073/PNAS.1400709111.

55. Chang, C.J., Mitra, K., Koya, M., Velho, M., Desprat, R., Lenz, J., and Bouhassira, E.E. (2011). Production of Embryonic and Fetal-Like Red Blood Cells from Human Induced Pluripotent Stem Cells. PLoS One *6*, e25761. https://doi.org/10.1371/JOURNAL.PONE.0025761.

56. Mattei, C., Lim, R., Drury, H., Nasr, B., Li, Z., Tadros, M.A., D'Abaco, G.M., Stok, K.S., Nayagam, B.A., and Dottori, M. (2019). Generation of vestibular tissue-like organoids from human pluripotent stem cells using the rotary cell culture system. Front. Cell Dev. Biol. *7*, 25. https://doi.org/10.3389/FCELL.2019.00025/BIBTEX.

57. Spence, J.R., Mayhew, C.N., Rankin, S.A., Kuhar, M.F., Vallance, J.E., Tolle, K., Hoskins, E.E., Kalinichenko, V.V., Wells, S.I., Zorn, A.M., et al. (2011). Directed differentiation of human pluripotent stem cells into intestinal tissue in vitro. Nature *470*, 105–109. https://doi.org/10.1038/NATURE09691.

58. Muffat, J., Li, Y., Yuan, B., Mitalipova, M., Omer, A., Corcoran, S., Bakiasi, G., Tsai, L.H., Aubourg, P., Ransohoff, R.M., and Jaenisch, R. (2016). Efficient derivation of microglia-like cells from human pluripotent stem cells. Nat. Med. *22*, 1358–1367. https://doi.org/10.1038/nm.4189.

59. Funakoshi, S., Fernandes, I., Mastikhina, O., Wilkinson, D., Tran, T., Dhahri, W., Mazine, A., Yang, D., Burnett, B., Lee, J., et al. (2021). Generation of mature compact ventricular cardiomyocytes from human pluripotent stem cells. Nat. Commun. *12*, 3155. https://doi.org/10.1038/S41467-021-23329-Z.

60. Johnston, Z.C., Bellingham, M., Filis, P., Soffientini, U., Hough, D., Bhattacharya, S., Simard, M., Hammond, G.L., King, P., O'Shaughnessy, P.J., and Fowler, P.A. (2018). The human fetal adrenal produces cortisol but no detectable aldosterone throughout the second trimester. BMC Med. *16*, 23. https://doi.org/10.1186/S12916-018-1009-7.

61. Perdomini, M., Dos Santos, C., Goumeaux, C., Blouin, V., and Bougnères, P. (2017). An AAVrh10-CAG-CYP21-HA vector allows persistent correction of 21-hydroxylase deficiency in a Cyp21 -/- mouse model. Gene Ther. *24*, 275–281. https://doi.org/10.1038/GT.2017.10.

62. Eclov, R.J., Lewis, T.E.W., Kapadia, M., Scott, D.W., McCoy, D.D., Rouse, J.L., Romero, K.B., Beard, C.W., and Mansfield, G.S. (2020). OR25-01 Durable CYP21A2 Gene Therapy in Non-Human Primates for Treatment of Congenital Adrenal Hyperplasia. J. Endocr. Soc. *4*. https://doi.org/10.1210/JENDSO/BVAA046.899.

63. Milenkovic, T., Zdravkovic, D., Savic, N., Todorovic, S., Mitrovic, K., Koehler, K., and Huebner, A. (2010). Triple A syndrome: 32 years experience of a single centre (1977-2008). Eur. J. Pediatr. *169*, 1323–1328. https://doi.org/10.1007/S00431-010-1222-7.

64. Handschug, K., Sperling, S., Yoon, S.J., Hennig, S., Clark, A.J., and Huebner, A. (2001). Triple A syndrome is caused by mutations in AAAS, a new WD-repeat protein gene. Hum. Mol. Genet. *10*, 283–290. https://doi.org/10.1093/HMG/10.3.283.

65. Bizzarri, C., Benevento, D., Terzi, C., Huebner, A., and Cappa, M. (2013). Triple A (Allgrove) syndrome: An unusual association with syringomyelia. Ital. J. Pediatr. *39*, 39. https://doi.org/10.1186/1824-7288-39-39/FIGURES/2.

66. Cronshaw, J.M., Krutchinsky, A.N., Zhang, W., Chait, B.T., and Matunis, M.J. (2002). Proteomic analysis of the mammalian nuclear pore complex. J. Cell Biol. *158*, 915–927. https://doi.org/10.1083/JCB.200206106.

67. Hirano, M., Furiya, Y., Asai, H., Yasui, A., and Ueno, S. (2006). ALADIN-NI482S causes selective failure of nuclear protein import and hypersensitivity to oxidative stress in triple A syndrome. Proc. Natl. Acad. Sci. USA *103*, 2298–2303. https://doi.org/10.1073/PNAS.0505598103.

68. Storr, H.L., Kind, B., Parfitt, D.A., Chapple, J.P., Lorenz, M., Koehler, K., Huebner, A., and Clark, A.J.L. (2009). Deficiency of ferritin heavy-chain nuclear import in triple a syndrome implies nuclear oxidative damage as the primary disease mechanism. Mol. Endocrinol. *23*, 2086–2094. https://doi.org/10.1210/ME.2009-0056.

69. Roucher-Boulez, F., Brac de la Perriere, A., Jacquez, A., Chau, D., Guignat, L., Vial, C., Morel, Y., Nicolino, M., Raverot, G., and Pugeat, M. (2018). Triple-A syndrome: a wide spectrum of adrenal dysfunction. Eur. J. Endocrinol. *178*, 199–207. https://doi.org/10.1530/EJE-17-0642.

70. Collares, C.V.A., Antunes-Rodrigues, J., Moreira, A.C., Franca, S.N., Pereira, L.A., Soares, M.M.S., Elias Junior, J., Clark, A.J., De Castro, M., and Elias, L.L.K. (2008). Heterogeneity in the molecular basis of ACTH resistance syndrome. Eur. J. Endocrinol. *159*, 61–68. https://doi.org/10.1530/EJE-08-0079.

71. Krumbholz, M., Koehler, K., and Huebner, A. (2006). Cellular localization of 17 natural mutant variants of ALADIN protein in triple A syndrome - shedding light on an unexpected splice mutation. Biochem. Cell. Biol. *84*, 243–249. https://doi.org/10.1139/O05-198.

72. Edie, S., Zaghloul, N.A., Leitch, C.C., Klinedinst, D.K., Lebron, J., Thole, J.F., McCallion, A.S., Katsanis, N., and Reeves, R.H. (2018). Survey of Human Chromosome 21 Gene Expression Effects on Early Development in Danio rerio. G3 (Bethesda) *8*, 2215–2223. https://doi.org/10.1534/G3.118.200144.

73. Sancak, Y., Peterson, T.R., Shaul, Y.D., Lindquist, R.A., Thoreen, C.C., Bar-Peled, L., and Sabatini, D.M. (2008). The Rag GTPases bind raptor and mediate amino acid signaling to mTORC1. Science *320*, 1496–1501. https://doi.org/10.1126/SCIENCE.1157535.

74. Pignatti, E., Leng, S., Yuchi, Y., Borges, K.S., Guagliardo, N.A., Shah, M.S., Ruiz-Babot, G., Kariyawasam, D., Taketo, M.M., Miao, J., et al. (2020). Beta-Catenin Causes Adrenal Hyperplasia by Blocking Zonal Transdifferentiation. Cell Rep. *31*, 107524. https://doi.org/10.1016/J.CELREP.2020.107524.

75. Livak, K.J., and Schmittgen, T.D. (2001). Analysis of Relative Gene Expression Data Using Real-Time Quantitative PCR and the $2^{-\Delta\Delta CT}$ Method. Methods *25*, 402–408. https://doi.org/10.1006/meth.2001.1262.

76. Seidel, E., Walenda, G., Messerschmidt, C., Obermayer, B., Peitzsch, M., Wallace, P., Bahethi, R., Yoo, T., Choi, M., Schrade, P., et al. (2020). Generation and characterization of a mitotane-resistant adrenocortical cell line. Endocr. Connect. *9*, 122–134. https://doi.org/10.1530/EC-19-0510.

77. Peitzsch, M., Dekkers, T., Haase, M., Sweep, F.C.G.J., Quack, I., Antoch, G., Siegert, G., Lenders, J.W.M., Deinum, J., Willenberg, H.S., and Eisenhofer, G. (2015). An LC–MS/MS method for steroid profiling during adrenal venous sampling for investigation of primary aldosteronism. J. Steroid Biochem. Mol. Biol. *145*, 75–84. https://doi.org/10.1016/J.JSBMB.2014.10.006.

78. Rodríguez-Asiain, A., Ruiz-Babot, G., Romero, W., Cubí, R., Erazo, T., Biondi, R.M., Bayascas, J.R., Aguilera, J., Gómez, N., Gil, C., et al. (2011). Brain Specific Kinase-1 BRSK1/SAD-B associates with lipid rafts: modulation of kinase activity by lipid environment. Biochim. Biophys. Acta *1811*, 1124–1135. https://doi.org/10.1016/j.bbalip.2011.10.004.

STAR★METHODS

KEY RESOURCES TABLE

REAGENT or RESOURCE	SOURCE	IDENTIFIER
Antibodies		
See Table S3 for all antibodies used in this study	This paper	Table S3
Bacterial and virus strains		
Lentivirus were generated as described in Material and Methods.	This paper	
pLJM1-MC2R-MRAP-Puro	This paper	N/A
pCMVdR8.2	Addgene	12260
pMD2.G	Addgene	12259
Biological samples		
FFPE and frozen samples of human adrenals	HCB-IDIBAPS Biobank	https://www.clinicbarcelona.org/en/idibaps/core-facilities/biobank
Human embryonic and fetal tissues	Human Developmental Biology Resource	www.hdbr.org/
Chemicals, peptides, and recombinant proteins		
FGF2	Peprotech	#100-18B
CHIR99021	TOCRIS	4423
Retinoic acid	R&D Systems	0695/50
BMP4	Peprotech	120–05
Y27632	TOCRIS	1254
Critical commercial assays		
ELISA Cortisol Saliva	Tecan	RE52611
ELISA Cortisol	Tecan	RE52061
Deposited data		
Raw and analyzed data	This paper	GEO: GSE224874
Fetal-Adrenal-Gland2: 12 weeks male		GSM4008675
Fetal-Adrenal-Gland3: 14 weeks male		GSM4008676
Fetal-Adrenal-Gland4: 12 weeks male		GSM4008677
Neonatal-Adrenal-Gland1-1		GSM4008720
Neonatal-Adrenal-Gland1-2		GSM4008721
F2: 8 weeks		GSM4088785
F7: 8 weeks		GSM4088786
Hs#19 [Adrenal]		GSM5815989
Hs#20 [Adrenal]		GSM5815990
Experimental models: Cell lines		
H9 hESCs	WiCell	WA09
H1 hESCs	WiCell	WA01
HEK293T	ATCC	CRL-11268
KOLF2	HipSci	HPSI0114i-kolf_2
ACS-1101 and BJFF	Washington University Kidney Translational Research Center	N/A
Experimental models: Organisms/strains		
Human: Passage 38 H9 and H1 ES cells	WiCell	www.wicell.org
Human: KOLF2, ACS-1101 and BJFF iPSCs lines	HipSci and Washington University	https://www.hipsci.org/ https://wustl.edu/
Human: HEK293T	ATCC	https://www.atcc.org/

(Continued on next page)

Continued		
REAGENT or RESOURCE	SOURCE	IDENTIFIER
Oligonucleotides		
See Table S4	This paper	Table S4
Recombinant DNA		
pLJM1-MC2R-MRAP-Puro	This paper	N/A
Software and algorithms		
GraphPad Prism 7		www.graphpad.com/
R v4.1.2 with Rstudio GUI (vRStudio 2022.07.0)		cran.r-project.org

RESOURCE AVAILABILITY

Lead contact

Further information and requests for resources and reagents should be directed to and will be fulfilled by the lead contact, Gerard Ruiz Babot (gerard.ruiz-babot@uniklinikum-dresden.de).

Materials availability

Plasmids generated in this study are available upon request.

Data and code availability

- Sequencing data have been deposited in GEO with the accession code GEO: GSE224874. Datasets used in this manuscript can be found in GEO: GSM4008675 (Fetal-Adrenal-Gland2: 12 weeks male); GEO: GSM4008676 (Fetal-Adrenal-Gland3: 14 weeks male); GEO: GSM4008677 (Fetal-Adrenal-Gland4: 12 weeks male); GEO: GSM4008720 (Neonatal-Adrenal-Gland1-1); GEO: GSM4008721 (Neonatal-Adrenal-Gland1-2); GEO: GSM4088785 (F2: 8 weeks); GEO: GSM4088786 (F7: 8 weeks); GEO: GSM5815989 (Hs#19 [Adrenal]) and GEO: GSM5815990 (Hs#20 [Adrenal]).
- This study does not report original code.
- Any additional information required to reanalyze the data reported in this paper is available from the lead contact upon request.

EXPERIMENTAL MODEL AND STUDY PARTICIPANT DETAILS

Cell culture

Human embryonic stem cells (hESCs)

H9 and H1 hESCs lines were maintained in StemFitBasic02 (Amsbio #SFB-500) supplemented with FGF2 10 ng/mL (Peprotech, #100-18B) and 1% Penicillin-Streptomycin (P/S, Thermo Scientific 15140122) in tissue culture plates coated with 1% v/v LDEV-Free hESC-qualified Geltrex (Life Technologies, #A1413302) in a 37°C incubator with 5% CO_2. For passaging, hESCs were dissociated using Accutase (StemCell Technologies, #07920) once per week and plated in medium containing FGF2, P/S and 10 µM Y27632 (ROCK inhibitor, TOCRIS, #1254). Medium was replaced on Monday and Wednesday. H9 and H1 were purchased from WiCell.

Induced pluripotent stem cells (iPSCs)

ACS-1101 and BJFF iPSCs lines were maintained in StemFitBasic02 supplemented with FGF2 10 ng/mL and 1% P/S in tissue culture plates coated with 1% Geltrex in a 37°C incubator with 5% CO_2. For passaging, iPSCs were dissociated using Accutase once per week and plated in medium containing FGF2, P/S and 10 µM Y27632. Medium was replaced on Monday and Wednesday. ACS-1101 and BJFF were obtained from the Washington university Kidney Translational Research Center.

For AAAS experiments, KOLF2 (ID: HPSI0114i-kolf_2), was obtained from HipSci (Human Induced Pluripotent Stem Cell Initiative; www.hipsci.org). This cell line was subcloned and karyotyped by FISH (Fluorescence *in situ* hybridization) prior to genome editing experiments. The subline, KOLF2-C1, was used for the tissue culture experiments described herein. Both the parental KOLF2 and KOLF2-C1 subline have a normal 46; XY karyotype (Koutsourakis, Bushell & Skarnes; unpublished data).

Cell lines

HEK293T were cultured with DMEM high glucose (D6429 Sigma), 10% FBS (16000-044 Gibco) and 1% P/S and NCI-H295R were cultures with Advance DMEM F12 (12634-010 Gibco), 1% ITS (Corning 354350), 2.5% Nu-Serum (Corning 355100) and 1% P/S.

Human samples

HDBR

Human embryonic and fetal tissues were obtained from the MRC/Wellcome-Trust funded Human Developmental Biology Resource (HDBR, http://www.hdbr.org/). Samples were collected with appropriate maternal written consent and with approval from the NRES

Committee North East - Newcastle and North Tyneside 1 (REC ref. 08/H0906/21 + 5) and NRES Committee London-Fulham (REC ref. 08/H0712/34 + 5). Embryonic specimens included 6 male and 10 female individuals at Carnegie stages 15–21. Fetal samples were collected from 9 males and 6 females at 14- and 18-week post-conception (pcw).

Barcelona biobank
FFPE and frozen samples of human adrenals were obtained from the HCB-IDIBAPS Biobank (registration number B.0000575), Hospital Clínic de Barcelona. Samples were obtained with the approval from the Ethical committee of the Hospital Clínic de Barcelona. Normal adult adrenal tissue samples were obtained from 16 males and 17 females aged 46 to 83 years, with biopsies conducted between 1997 and 2004.

METHOD DETAILS

Antibodies
The antibodies used in this study can be found in Table S3.
   Primers: PCR, qPCR and cloning primers.
   Primers used in this study can be found in Table S4.

Generation of CRISPR-Cas9 genome engineered lines
To knockout the function of AAAS, the biallelic targeting strategy was to replace one copy of exon 2 with a puromycin (puro) selection cassette by homologous recombination (HR) and simultaneously damage the other allele by non-homologous end-joining.

To generate the point mutation 43C>A in the AAAS locus, KOLF2_C1 cells were co-transfected with preassembled Cas9-RNP and ssODN containing the C>A point mutation for its introduction into genomic DNA by homology-directed repair (HDR). The ssODN was symmetric containing 50-base homology arms on either side of the C>A point mutation. The ssODN was non-complementary to the CRISPR gRNA oligo to prevent it from annealing to the gRNA. In order to obtain homozygotes, the experiment was repeated by re-transfecting the heterozygotes.

Generation of pLJM1-MC2R-MRAP-Puro vector
MRAP_pCSdest was a gift from Roger Reeves (Addgene plasmid # 53833; http://n2t.net/addgene:53833; RRID: Addgene_53833)[72] and pUltra-Chili was a gift from Malcolm Moore (Addgene plasmid # 48687; http://n2t.net/addgene:48687; RRID: Addgene_48687). pLJM1-EGFP was a gift from David Sabatini (Addgene plasmid # 19319; http://n2t.net/addgene:19319; RRID: Addgene_19319).[73] The MRAP ORF was subcloned into the vector pUltra-Chili using NheI and EcoRI and the MC2R ORF was PCR amplified from a human adrenal cDNA sample and subcloned in the pUltra-Chili vector using AgeI and BamHI. MC2R-2A-MRAP was subsequently subcloned into pLJM1-EGFP vector using AgeI and EcoRI.

Lentivirus production
Lentiviral particles were prepared using 90% confluent HEK293T cells. For each 10-cm dish, cells were transfected with pCMV-MC2R-MRAP (10 μg) vector together with the packaging vectors pCMVdR8.2 (3.2 μg) and pMD2.G (1.8 μg) using 100 μL of 1 mg/ml polyethyleneamine reagent (PEI, Warrington, USA). 2 h after transfection medium was replaced to DMEM, 10%FBS (v/v), 1% P/S. After 24 h, medium was changed to Advanced RPMI 1640, 1% Glutamax and 1% P/S. Medium was collected after 24 and 48 h, filtered, aliquoted and immediately stored at frozen at −80°C.

Cell differentiation
15,000 cells/well were plated in a 24-well plate coated with 1% Geltrex in StemFit Basic02 supplemented with FGF2 10 ng/mL, Y27632 10 μM and 1% P/S. After 72 h medium was replaced to Advanced RPMI 1640, 1% Glutamax and 1% P/S (Diff. medium) supplemented with CHIR99021 3 μM (TOCRIS, #4423) for 2 days and medium was refreshed for 24 h (total of 3 days). At day 3 of differentiation, medium was changed to Diff. medium supplemented with retinoic acid 1–10 μM (R&D Systems, 0695/50) for 24 h. At day 4 and 5, medium was changed to Diff. medium supplemented with BMP4 1–10 μM (Peprotech, 120-05) for a total of 48 h. At day 6, cells were detached using Accutase, 500,000 cells/well were plated in a well of a 6-well plate coated with 1% Geltrex in Diff. medium and Y27632 10 μM, and infected with 1.5 μL at 1×10^{12} gc/ml of SF-1/RFP virus. Medium was changed 24 h after infection to Diff. Medium and cell lines were established. When indicated, cells were treated with different concentrations of br-cAMP in the medium for 48 h.

For generation of hiSCs-MM lines, lentiviral particles were obtained as described in the "lentiviral production" section and 1 mL of HEK293T cell supernatant was incubated with 500,000 hiSCs. Medium was changed after 24 h and puromycin was used to select transduced cells after 24 h.

Immunocytochemistry
hPSCs at different days of differentiation were fixed using 4% paraformaldehyde in PBS for 20 min on ice. Permeabilization was performed using PBS containing 0.02% saponin for 7 min followed by 15 min with PBS with 10 mM glycine and 0.01% saponin. Cells were blocked for 1 h with PBS containing 0.01% saponin, 10 mM glycine and 5% (w/v) BSA (Sigma, #05470) before incubation with

primary antibodies (dilution 1:25 to 1:100) in PBS containing 0.01% saponin and 1% BSA (buffer A) overnight. Cells were incubated for 45 min with the corresponding secondary antibodies (Thermo Fisher Scientific) diluted 1:400 in buffer A and nuclei were stained using DAPI (4′,6-diamidino-2-phenylindole) (Thermo Fisher Scientific, #D1306). Images were obtained with the fluorescence microscope EVOS FL Auto 2 Imaging System.

Immunohistochemistry

Five μm-thick sections were obtained from the Human Developmental Biology Resource (HDBR-UK) and processed for immunostaining, as previously described.[74] Briefly, sections were rinsed successively in xylene, an ethanol gradient (100%–50%) and PBS. Antigen retrieval was performed by boiling the samples for 10 min in Tris-EDTA pH9 (1.21g Tris Base +0.37 g EDTA +0.05% Tween 20 in 1L H_2O). Sections were blocked in 10% Normal Goat Serum (NGS), 0.5% BSA, 0.3% Tween 20 in PBS for 1 h at RT in a humidified chamber. Primary antibodies were diluted 1:100 in 1% NGS, 0.5% BSA in PBS overnight at 4C in the humidified chamber. Slides were washed, incubated with secondary antibody (1/400) and DAPI (1:1.000) in 1% NGS, 0.5% BSA for 1 h and mounted in ProLong Gold Antifade Mountant Solution (Thermo Fisher, #P36930)

Gene expression analysis

Messenger RNA was purified using TRIReagent (Sigma, #T9424) using the Direct-zolTM RNA kit (Zymo Research), following the manufacturer's instructions. cDNA was obtained using 10–500 ng of mRNA with the High-Capacity cDNA Reverse Transcription Kit (Thermo fisher, #4368814) for 10 min at 25°C, 90 min at 42°C and 15 min at 70°C. Samples were diluted to a final concentration of 2 ng/mL and 2 ng of cDNA were used for PCR amplification.

Standard PCR experiments were performed using Taq DNA polymerase (NEB, M0273). SYBR FAST Universal Kit (KAPA Biosystems, #KK4602) and 500 nM forward and reverse primers were used for Real Time quantitative PCR (RTqPCR) using a QuantStudio 6 Flex thermocycler (Thermo fisher). Relative quantification analysis was performed following the $2^{-\Delta\Delta CT}$ method[75] and data was normalized to Actb expression.

Hormone quantification

Supernatants of differentiated hPSCs at different time points were collected and quantification of metabolites was assayed by mass spectrometry or ELISA.

ELISA

Hormones were measured using the following kits: Cortisol Saliva (Tecan, RE52611) and cortisol (Tecan, RE52061) according to the manufacturer's instructions.

LC-MS/MS procedure

Steroid hormones progesterone, 11-deoxycorticosterone, corticosterone, 11-dehydrocorticosterone, aldosterone, 17-hydroxyprogesterone, 11-deoxycortisol, cortisol, cortisone, dehydroepiandrosterone, androstenedione and testosterone were simultaneously analyzed by liquid chromatography-tandem mass spectrometry (LC-MS/MS) as described elsewhere.[76,77]

Transmission electron microscopy

Samples were fixed overnight in a mixture of 1.25% formaldehyde, 2.5% glutaraldehyde, and 0.03% picric acid in 0.1 M sodium cacodylate buffer, pH 7.4. The fixed tissues were washed with 0.1M sodium cacodylate buffer and post-fixed with 1% osmium tetroxide/1.5% potassium ferrocyanide (in H2O) for 2 h. Samples were then washed in a maleate buffer and post fixed in 1% uranyl acetate in maleate buffer for 1 h. Tissues were then rinsed in ddH₂0 and dehydrated through a series of ethanol (50%, 70%, 95%, (2x)100%) for 15 min per solution. Dehydrated tissues were put in propylene oxide for 5 min before they were infiltrated in epon mixed 1:1 with propylene oxide overnight at 4C. Samples were polymerized in a 60°C oven in epon resin for 48 h. They were then sectioned into 80nm thin sections and imaged on a JEOL 1200EX Transmission Electron Microscope.

Bioinformatic analysis

Library preparation and sequencing for bulk RNA seq

Libraries were prepared using Roche Kapa mRNA HyperPrep strand specific sample preparation kits from 200ng of purified total RNA according to the manufacturer's protocol on a Beckman Coulter Biomek i7. The finished dsDNA libraries were quantified by Qubit fluorometer and Agilent TapeStation 4200. Uniquely dual indexed libraries were pooled in equimolar ratios and shallowly sequenced on an Illumina MiSeq to further evaluate library quality and pool balance. The final pool was sequenced on an Illumina NovaSeq 6000 targeting 40 million 150bp read pairs per library at the Dana-Farber Cancer Institute Molecular Biology Core Facilities.

Single cell datasets

Single cell datasets used in this work were obtained from the following public databases.[49,50,53] Accession numbers and GEO Sample name and description can be found in Table 3.

Single-cell RNA-seq analysis

Matrix of raw counts were downloaded from GEO accessions and imported to R v4.1.2 with Rstudio GUI (vRStudio 2022.07.0). Single-cell matrices were imported to R (v4.2.1) using Seurat (v4.1.1) [https://doi.org/10.1038/nbt.3192]. The global-scaling normalization technique "LogNormalize" was used to normalize the UMI count matrix. Seurat package's "ScaleData" function was used to remove the unwanted sources of variation (UMI coverage and amount of ribosomal genes per cell). After identify the cluster with "FindClusters" function, the "RunUMAP" function was used to non-linear dimensional reduction. To annotate the clusters generated, differentially expressed features were identified by looking at the markers differing between clusters using the function "FindAllMarkers". This allow the identification of each cluster by associating the differentially expressed genes to canonical genes belonging to specific cellular cell types. Plots were generated with different custom modifications of Seurat functions DimPlot, VlnPlot, FeaturePlot, and ggplot2.

Bulk matrix of counts

Bulk RNA sequencing was performed at the Molecular Biology Core Facilities (MBCF) at Dana-Farber Cancer Institute. Raw paired-end fastq files were preprocessed to remove the low quality reads using TrimGalore v0.6.6 (cutadapt v1.18) using a default Quality Phred score cutoff of 20. Quality control of the reads was performed prior and after trimming using fastQC v0.11.9 and multiQC v1.11. Validated reads were aligned using Star v2.7.9a against human reference genome and the annotation GTF file (GRCh38.p13) from Gencode v39 primary assembly. The strandness of the libraries was determined using Rseq v4.0.0 and BEDOPS v2.4.4 tools and the script infer-experiment.py. The final matrix of raw counts was formatted using R v4.1.2 and Rstudio GUI.

Pseudobulking and bulk clustering analysis

Pseudo-bulk count matrix was generated with the common genes of the scRNAseq samples by adding the processed single-cell counts in R, obtaining a matrix of counts. This pseudo-bulk count matrix was merged with the bulk data, imported to DESEq2 and normalized. Variance stabilizing transformation was used prior to visualization on PCA plots.

Nile Red Staining

Nile Red staining was performed on cells using the Nile Red Staining kit (ab228553, Abcam), following the manufacturer's instructions.

WB analysis

Immunoblotting was performed as described previously with minor modifications.[78] Briefly, proteins were resolved by SDS-PAGE (Biorad, USA) and transferred to Roti-PVDF membranes (Carl Roth GmbH, Germany). Membranes were blocked with TBS-T (20 mM Tris–HCl pH 7.6, 150 mM NaCl, 0.1% Tween 20) containing 5% skimmed milk, and incubated with the appropriate antibody. Detection was performed by incubating with an appropriate horseradish peroxidase-conjugated secondary antibody (Biorad, USA) and SuperSignal West Pico PLUS chemiluminescence reagent (Thermo Scientific, USA).

Data analysis

Figures and tables were generated using GraphPad, Microsoft Excel, ImageJ and PowerPoint. We used the green bar throughout the manuscript to depict the column used for comparison to other bars.

QUANTIFICATION AND STATISTICAL ANALYSIS

Statistical analysis was performed using GraphPad Prism 7 and statistical significance was determined using one-way ANOVA followed by Dunnet's multiple comparison test correction. Student's t test analysis was performed when only two means were compared. Significance $p > 0.05$ ns; $p < 0.05$ *; $p < 0.01$ **; $p < 0.001$ ***; $p < 0.0001$ ****.